UNIVERSITY OF CALIFORNIA
RIVERSIDE

Majorana Zero Modes in Superconducting Rings and Arrays

A Dissertation submitted in partial satisfaction
of the requirements for the degree of

Doctor of Philosophy

in

Physics

by

Ali Beyramzadeh Moghadam

December 2016

Dissertation Committee:

Dr. Kirill Shtengel, Chairperson
Dr. Vivek Aji
Dr. Leonid Pryadko

The Dissertation of Ali Beyramzadeh Moghadam is approved:

Committee Chairperson

University of California, Riverside

Acknowledgments

Firstly, I would like to express my sincere gratitude to my advisor Prof. Shtengel for the continuous support of my Ph.D study and related research, for his patience, motivation, and immense knowledge. His guidance helped me in all the time of research and writing of this thesis.

Besides my adviser, I would like to thank my fellow students and friends Amir, Jack, Shima, Gonca, Harris, David, Yafis, Shooby, Irene, Hooshang, Behnam and Mostafa for their support and valuable friendship and also useful discussions and valuable feedback.

Last, but not least, I would like to thank my family for supporting me spiritually throughout writing this thesis and my my life in general.

This work was supported by NSF Grant No. DMR-1411359.

To my brother, Kavian.

ABSTRACT OF THE DISSERTATION

Majorana Zero Modes in Superconducting Rings and Arrays

by

Ali Beyramzadeh Moghadam

Doctor of Philosophy, Graduate Program in Physics
University of California, Riverside, December 2016
Dr. Kirill Shtengel, Chairperson

Majorana zero modes are zero energy excitations with unusual (non-Abelian) statistics that offer a promising platform for quantum computation. These modes are theoretically expected to exist in a variety of physical systems, most prominently in chiral p-wave superconductors. In the case of a spinless (or spin-polarized) superconductor, a conventional vortex – a topological defect that carrying one quantum of superconducting magnetic flux – would host such a zero mode. In the presence of spin degrees of freedom, however, such a mode would require a half quantum vortex, i.e. a vortex characterized by a half-integer number of the superconducting flux quanta. To guarantee the single-valued nature of the order parameter, a non-trivial spin texture is required, which would allow the order parameter to pick up an additional factor of -1 around the vortex.

Half-integer flux quantization has been observed in mesoscopic rings of superconducting Sr_2RuO_4. This finding suggests a chiral $p + ip$ nature of the superconducting order parameter. Under the assumption that the d-vector (which parametrizes the triplet pairing) lies in the plane of a 2D superconductor, such rings are expected to support Majorana zero modes at their inner and outer edges. However, such modes have not been directly observed in experiments. More recently,

H.-Y. Kee and M. Sigrist argued that the spin-orbit coupling in such systems can stabilize a different spin texture, also consistent with half quantum vortices. That spin texture is characterized by the presence of a so-called d-soliton –a radial domain wall between the regions where the d-vector is oriented in the positive and negative z-directions.

Our theoretical investigation of superconducting rings with d-solitons confirms the existence of two Majorana zero modes, one at each boundary. Furthermore, the presence of a d-soliton alter the hybridization between the localized Majorana modes at the inner and outer boundaries.

In addition to chiral p-wave superconductors, some index theorem-like arguments can be used to predict Majorana zero modes in an array of vortices in chiral d-wave superconductors, our numerical studies did not produce any evidence of Majorana zero modes in such systems.

Contents

List of Figures

Chapter 1

Introduction

Recently Majorana zero modes have been attracting a lot of attention,[1–3] both theoretical and experimental, due to their unusual property – the non-Abelian braiding statistics.[4] As a result, they offer a promising platform for topological quantum computation.[5–7] One of the physical systems predicted to support these zero modes is a chiral $p + ip$ superconductor.[8,9] If such a superconductor is effectively spinless (e.g., by the virtue of being spin-polarized), a Majorana zero mode is bound to a vortex core. The presence of the spin degree of freedom, however, makes this situation more interesting and complex. In this case Majorana zero modes are hosted by half quantum vortices, i.e. vortices where the phase of the superconducting order parameter winds by π (instead of 2π) around the vortex core. The required single-valued nature of the order parameter is ensured by a concomitant π-rotation of the spin quantization axis.[4]

Experimental search for half quantum vortices has been motivated by the suggestion that the superconducting state in Sr_2RuO_4 may be described by the chiral p-wave order parameter.[10] However, isolated half quantum vortices have not been seen in the bulk material. A possible rea-

son for their absence is that they may be energetically unfavorable in comparison to full quantum vortices. This is because the spin current associated with a half quantum vortex is not screened at large distances, unlike the conventional supercurrent.[11] This consideration would rule out their existence in bulk samples. However, this still leaves us with two physical scenarios for realizing half quantum vortices. Firstly, there is a possibility for their existence in compound objects, whereby two half quantum vortices with opposite spin windings are paired together, thus canceling the spin currents at large distances. The second, more interesting scenario can be realized by simply enforcing a physical cutoff for those currents, which would naturally happen in a mesoscopic sample. It is therefore likely that this second possibility is in fact realized in mesoscopic rings where the observation of half-height magnetization steps has been reported by Jang et al.[12] However, there is no direct evidence of Majorana zero modes in these systems, even though one would naïvely expect their existence whenever the flux through a ring is a half of the superconducting flux quantum. Whether or not such Majorana zero modes actually exist in these rings is an interesting question in light of the resent model put forward by Kee and Sigrist[13] which proposes a different spin texture for half quantum vortices in these experiments, compared to the one for which the existence of zero modes had been theoretically established.[4]

In chapter two we review the basic concepts of superconductivity and introduce vortices in type II superconductors and further we discuss the presence of excitation that are bonded to the core of vortex while we focus on the low energy behavior of such states. Moreover, we talk about spinless $p + ip$ superconductors and their role to observe Majorana zero modes. We solve the Bogoliubov-de Gennes(BdG) equations exactly for zero energy to demonstrate the behavior of Majorana zero modes in this chirality. Afterwards, we study the topological characteristic of

different phases and we show that only in topologically non-trivial phases Majorana zero modes can be observed. we conclude the chapter by moving to spinful superconductors and effect of spin on Majorana zero modes.The goal of chapter three is to demonstrate the existence of Majorana zero modes in the model introduced by Kee and Sigrist. We will use numerical methods to solve BdG equations in this model. In chapter four using the exact solution we found in chapter two we study the energy splitting between two Majorana modes due to their hibridization across a narrow ring. In chapter five, we look at a completely different problem to see if it is possible to observe Majorana zero modes in d-wave superconductor.

Chapter 2

Low energy behavior of states bonded to the core of a vortex

In this chapter we briefly review the basic concepts of superconductivity while we focus on p-wave superconductors. Further we study the system in presence of vortices- a vortex is a topological defect exhibited in type II superconductors- and we also mention energy spectrum of the states that are bonded to a the core of a vortex. We will show that in the p-wave superconductors there are modes with zero energies that are localized around the vortex core. Moreover we studies the low energy behavior of such states and properties of their wavefunctions. Adding the pin to the mixture would make things a lot lore interesting which results in making these zero modes unstable. To stabilize, we look at the configuration of half quantum vortices and the energy spectrum's alternation.

2.1 s-wave superconductors

Most theories of superconductivity are based on a theory first introduced by Bardeen, Cooper and Schrieffer (BCS) in 1957.[14,15] The ground state can be presented as a Bose condensate of pairs of electrons. The BCS mean-field theory assumes a underlying attractive interaction between each pair of electrons. In s-wave superconductors the order parameter is taken to be a spherical symmetric function that links two opposite spins(up and down) to each other. The effective BCS Hamiltonian can be written as

$$H = \sum_{k\sigma} \left[\xi_k \, c^\dagger_{k\sigma} c_{k\sigma} + \left(\Delta^* \, c_{-k\downarrow} c_{k\uparrow} + \Delta \, c^\dagger_{k\uparrow} c^\dagger_{-k\downarrow} \right) \right] \tag{2.1}$$

where $\xi_k = \epsilon_k - \mu$, ϵ_k is the single-particle kinetic energy, μ is chemical potential, σ ($\uparrow$ or $\downarrow$) runs over spins and Δ is the order parameter for the s-wave superconductors. In order to simplify the notation we would employ the Nambu spinor representation

$$\Psi^\dagger_k = \begin{pmatrix} c^\dagger_{k\uparrow} & c_{-k\downarrow} \end{pmatrix}, \qquad \Psi_k = \begin{pmatrix} c_{k\uparrow} \\ c^\dagger_{-k\downarrow} \end{pmatrix} \tag{2.2}$$

and write the Hamiltonian as

$$H = \sum_k \Psi^\dagger_k \begin{pmatrix} \xi_k & \Delta \\ \Delta^* & -\xi_k \end{pmatrix} \Psi_k + \sum_k \xi_k \tag{2.3}$$

Using a so-called Bogoliubov (Unitary) transformation one can diagonalize the Hamiltonian (Eq. 2.3).

$$\begin{pmatrix} \gamma_{k\uparrow} \\ \gamma^\dagger_{-k\downarrow} \end{pmatrix} = \begin{pmatrix} u^*_k & v^*_k \\ v_k & -u_k \end{pmatrix} \begin{pmatrix} c_{k\uparrow} \\ c^\dagger_{-k\downarrow} \end{pmatrix} \tag{2.4}$$

Here the functions u_k and v_k are complex and to ensure Unitarity they should satisfy $|u_k|^2 + |v^2_k| = 1$, so that the new operators,$\gamma_{k,\sigma}$, obey fermionic commutation rules $\{\gamma_{k,\sigma}, \gamma^\dagger_{k',\sigma'}\} = \delta_{k,k'}\delta_{\sigma,\sigma'}$. The

diagonalized Hamiltonian can be written as

$$H = \sum_{k\sigma} E_k \gamma^\dagger_{k\sigma}\gamma_{k\sigma} + \sum_k (\xi_k - E_k) \tag{2.5}$$

with $E_k \geq 0$. Since the constant only shifts the energy we can drop it and determine the Hamiltonian with its commutation rules

$$[H, \gamma_{k\sigma}] = -E\,\gamma_{k\sigma} \tag{2.6}$$

$$[H, \gamma^\dagger_{k\sigma}] = E\,\gamma^\dagger_{k\sigma} \tag{2.7}$$

In order to find the solution for E_k, u_k and v_k one obtains Bogoliubov-de Gennes (BdG) equations

$$\begin{pmatrix} \xi_k & \Delta \\ \Delta^* & -\xi_k \end{pmatrix} \begin{pmatrix} u_k \\ v_k \end{pmatrix} = E_k \begin{pmatrix} u_k \\ v_k \end{pmatrix} \tag{2.8}$$

which result in

$$E_k = \sqrt{\xi^2 + |\Delta|^2} \tag{2.9}$$

$$v_k/u_k = (E_k - \xi_k)/\Delta \tag{2.10}$$

$$|u_k|^2 = \frac{1}{2}\left(1 + \frac{\xi_k}{E_k}\right) \tag{2.11}$$

$$|v_k|^2 = \frac{1}{2}\left(1 - \frac{\xi_k}{E_k}\right) \tag{2.12}$$

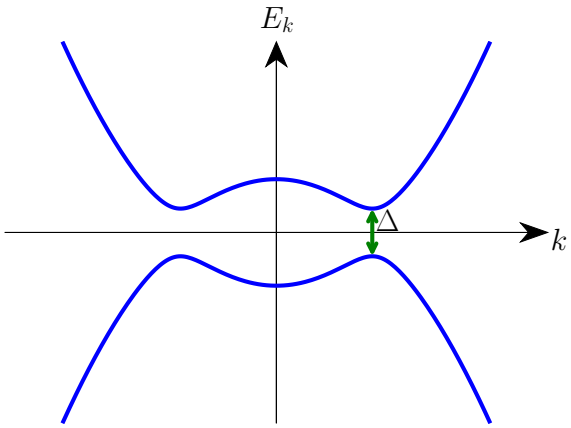

Figure 2.1: Energy spectrum of a s-wave superconductors, E_k, as a function of k

These equations would determine the functions u_k and v_k up to a phase which does not change any of the physics of the problem. Eq. 2.6 and Eq. 2.7 show that if there is a solution with energy E_k, its particle-hole symmetric counterpart has energy of $-E_k$.

Next we study the quasiparticle spectrum in the presence of vortices for s-wave superconductors. Vortices are topological defects which carry an integer flux quanta. In two dimensions a vortex can be considered as a small circle with vanishing density at the center. For such a system, the superconducting order parameter is given by

$$\Delta(\mathbf{r}) = e^{im\theta} f(r) \tag{2.13}$$

where r and θ are polar coordinates centered on the vortex, $f(r)$ is a real function of r that vanishes at the center and would take the mean-field value of superconducting order parameter (Δ_0) as $r \to \infty$ (see Fig. 2.2) and m is the winding number of the vortex (vorticity).

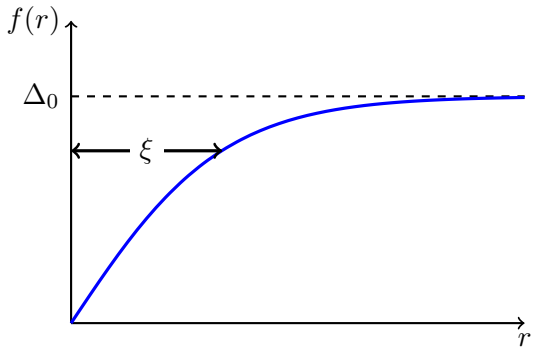

Figure 2.2: Superconducting order parameter profile in presence of a vortex has been simulated with $f(r) = \Delta_0 \tanh(\frac{r}{\xi})$ where Δ_0 is the mean-field value of superconducting order parameter and ξ is the vortex's core radius.

For winding number, $m = \pm 1$ one can write the BdG equations (Eq. 2.8) in real space as

$$\begin{pmatrix} -\frac{1}{2m}\nabla^2 - \mu & e^{i\theta} f(r) \\ e^{-i\theta} f(r) & \frac{1}{2m}\nabla^2 + \mu \end{pmatrix} \begin{pmatrix} u(\mathbf{r}) \\ v(\mathbf{r}) \end{pmatrix} = E \begin{pmatrix} u(\mathbf{r}) \\ v(\mathbf{r}) \end{pmatrix} \tag{2.14}$$

which are a set of two differential equations and can be solved exactly.[16] The low energy behavior

of the fermionic states bounded to the vortex core are quantized[16] as

$$E = (n + \frac{1}{2})\omega_0 \tag{2.15}$$

where n is related to the angular momentum of the fermionic states[8] and ω_0 is the level spacing which is much smaller than the energy gap, $\omega_0 \sim \Delta_0^2/E_F \ll \Delta_0$.

2.2 Majorana zero modes in the spinless $p + ip$ superconductors

Not long after BCS theory, it has been shown that the theory can also support non-zero relative angular momentum for paring electrons. While in general a l-paired state can have gapless point on its Fermi surface, one might find a particular pairing with completely gapped spectrum. Focusing on p-wave superconductors, one can show $p+ip$ order parameter would show the gapped states throughout the whole Fermi surface. In two dimensions, a spinless $p+ip$ superconductor can be modeled as

$$H = \int d^2\mathbf{r} \left\{ \psi^\dagger(-\frac{\nabla^2}{2m} - \mu)\psi - \frac{\Delta_0}{2}\left[e^{i\phi}\psi^\dagger\left(\partial_x + i\partial_y\right)\psi^\dagger + \text{ H.c.}\right]\right\} \tag{2.16}$$

where m is the effective mass, μ is the chemical potential and $\Delta_0 \geq 0$ is the p-wave pairing amplitude while ϕ is the superconducting phase. One should notice that here unit of Δ_0 in contrast to s-wave is energy $\times$ length. Here we take superconductivity order parameter to be uniform to find the bulk energy spectrum, though we relax this condition later when we talk about vortices. In a system with periodic boundary condition along both x and y axes (i.e. on a torus), one can diagonalize the Hamiltonian (Eq. 2.16) by going to momentum space. Defining $\Psi_{\mathbf{k}}^\dagger = (\, c_{\mathbf{k}}^\dagger \; c_{-\mathbf{k}} \,)$,

one would get

$$H = \frac{1}{2}\sum_{\mathbf{k}} \Psi_{\mathbf{k}}^{\dagger}\mathcal{H}_{\mathbf{k}}\Psi_{\mathbf{k}}$$

$$\mathcal{H}_{\mathbf{k}} = \begin{pmatrix} \xi(k) & -i\Delta_0 e^{i\phi}(k_x + ik_y) \\ i\Delta_0 e^{-i\phi}(k_x - ik_y) & -\xi(k) \end{pmatrix} \tag{2.17}$$

with $\xi(k) = (k^2/2m) - \mu$. A unitary transformation of form $\gamma_{\mathbf{k}} = u_{\mathbf{k}}c_{\mathbf{k}}^{\dagger} + v_{\mathbf{k}}c_{-\mathbf{k}}$ can diagonalize the matrix $\mathcal{H}_{\mathbf{k}}$ with energy eigenvalues of

$$E_{\text{bulk}}(k) = \pm\sqrt{\xi_k + \Delta_0^2 k^2} \tag{2.18}$$

and in terms of these quasiparticle operators the Hamiltonian can be written as

$$H = \sum_k E_{\text{bulk}}(k)\gamma_k^{\dagger}\gamma_k \, . \tag{2.19}$$

For any positive chemical potential the bulk is fully gaped ($E_{\text{gap}} = \Delta_0 k_F = \Delta_0\sqrt{2m|\mu|}$). As μ decreases, one can see that the gap closes at $\mu = 0$ due to the fact that Pauli exclusion prohibits p-wave pairing at $k = 0$. The gap would open again as we go to negative chemical potential. It has been shown that these two phases exhibit different topological phases.[1,9]

To expose the topological differences of these two regimes, we consider a two dimensional superconductor describe by a Hamiltonian of form[17]

$$\mathcal{H}(\mathbf{k}) = \mathbf{h}(\mathbf{k}) \cdot \boldsymbol{\sigma} \tag{2.20}$$

where $\mathbf{h}(\mathbf{k})$ is non-zero for all values of k. One can map the 2D momentum space to a unit sphere by defining a unit vector $\hat{\mathbf{h}}(\mathbf{k})$. The number of times that this map covers the entire unite sphere

defines *Chern number* which is topologically invariant. Formally one can write

$$C = \int \frac{d^2\mathbf{k}}{4\pi} \hat{\mathbf{h}} \cdot \left(\partial_{k_x} \hat{\mathbf{h}} \times \partial_{k_y} \hat{\mathbf{h}} \right) \tag{2.21}$$

the integrand measures the solid angle that $\hat{\mathbf{h}}(\mathbf{k})$ sweeps on the unit sphere. Taking the integral over the all $\mathbf{k}$ would give an integer that is invariant under deformations of $\hat{\mathbf{h}}(\mathbf{k})$ as long as the gap does not close. The Chern number can only change by closing the gap and making $\hat{\mathbf{h}}(\mathbf{k})$ ill-defied at some point in the momentum space.

Considering Hamiltonian in Eq. 2.17 by taking $\phi = 0$ (since we assumed ϕ is constant this can be done by a gauge transformation) we can determine that $h_z(\mathbf{k}) = \xi(k)$, $h_x(\mathbf{k}) = \Delta_0 k_y$ and $h_y(\mathbf{k}) = \Delta_0 k_x$. For $\mu < 0$ phase, ξ is always positive and therefore the unit vector $\hat{\mathbf{h}}(\mathbf{k})$ cannot sweep the lower hemisphere. One can conclude that the Chern number for negative chemical potential has to be zero which means this phase is topologically trivial state. On the other hand, for positive chemical potential the unit vector is pointing to the south pole at $k = 0$ ($\hat{\mathbf{h}}(0) = -\hat{z}$) and as we increase k it moves toward the to north pole when $k \to \infty$. By calculating the Chern number using Eq. 2.21 one obtains $C = -1$ for $p + ip$ superconductors which would prove that $\mu > 0$ has an non-trivial topological phase.[18–20]

Hamiltonian 2.16 can be diogonalized in the basis of quasiparticle operators $\gamma^\dagger = u\psi^\dagger + v\psi$. The corresponding BdG equations can be written as

$$[H, \gamma^\dagger] = E\gamma^\dagger. \tag{2.22}$$

Due to presence of particle-hole symmetry one can show that if $\gamma^\dagger$ is the solution for energy E there is solution of form γ with Energy $-E$. This would prove that zero modes (solutions with zero energy) are self-conjugate (Majorana) fermions

$$\gamma^\dagger(E = 0) = \gamma(E = 0) \tag{2.23}$$

We should mention that Majorana zero modes exhibit non-Abelian statistics[4] which would make them a useful platform for topological quantum computation. Next search for Majorana zero modes in different setups.

2.3 The exact solution for Majorana zero modes in the spinless $p + ip$ superconductors

It has been shown that for p-wave superconductors with odd vorticity one can construct a normalizable solution to support Majorana zero modes.[8,9] Here we will solve BdG differential equations exactly to show the behavior of the Majorana zero modes. As we promised earlier now we let order parameter to be a function of position and therefore we need to tweak Eq. 2.16 to be symmetric for order parameter. Using the properties of Majorana zero modes ($u = v^*$) one can write the BdG differential equations in real space as

$$-\frac{1}{2m}\nabla^2 u - \mu u - \sqrt{\Delta}\left(\partial_x + i\partial_y\right)\sqrt{\Delta}u^* = 0 \tag{2.24}$$

Order parameter is assumed to have vorticity of one,

$$\Delta_0 e^{i\theta} \tag{2.25}$$

where θ is the polar angle and further we assume that Δ_0 is constant everywhere except inside an infinitesimally small core.

With a unitary transformation of $u \to u\, e^{i\theta/2}$, Eq. 2.24 transforms to

$$\left(-\frac{1}{2m}\nabla^2 + \frac{1}{2mr^2} - \mu\right)u - \Delta_0\left(\partial_r + \frac{i}{r}\partial_\theta + \frac{1}{2r}\right)u^* = 0. \tag{2.26}$$

Further we assume that the solution is a spherically symmetric function $u(r)$, reducing Eq. 2.26 to

$$\left(-\frac{1}{2m}\partial_r^2 - \frac{1}{2mr}\partial_r + \frac{1}{2mr^2} - \mu\right) u - \Delta_0 \left(\partial_r + \frac{1}{2r}\right) u^* = 0. \tag{2.27}$$

Since $u(r)$ is a complex function, one can write it as $u(r) = u_1(r) + iu_2(r)$ and solve the differential equations for real and imaginary parts separately. The solution for the real part $u_1(r)$ is

$$u_1(r) = e^{-m\Delta_0 r} \begin{cases} c_1 J_1(r\alpha_+) + c_2 Y_1(r\alpha_+) & \mu > \frac{1}{2}m\Delta_0^2 \\ c_3 I_1(r\alpha_-) + c_4 K_1(r\alpha_-) & \mu < \frac{1}{2}m\Delta_0^2 \end{cases} \tag{2.28}$$

with

$$\alpha_+ = \sqrt{2m\mu - m^2\Delta_0^2}\ , \qquad \alpha_- = \sqrt{m^2\Delta_0^2 - 2m\mu}\quad .$$

where $J_1(r)$ and $Y_1(r)$ are Bessel functions of first and second kind respectively and $I_1(r)$ and $K_1(r)$ are modified Bessel functions. The only difference in the case of $u_2(r)$ is the sign of exponent;

$$u_2(r) = e^{m\Delta_0 r} \begin{cases} c_1 J_1(r\alpha_+) + c_2 Y_1(r\alpha_+) & \mu > \frac{1}{2}m\Delta_0^2 \\ c_3 I_1(r\alpha_-) + c_4 K_1(r\alpha_-) & \mu < \frac{1}{2}m\Delta_0^2 \end{cases} . \tag{2.29}$$

Since Y_1 and K_1 are not well-behaved at the origin we can put them aside for now and focus on the behavior of functions J_1 and I_1. In Fig 2.3[21] a sketch of u_1 and u_2 is plotted. One can notice that both solutions associated withu_2 are not normalizable and therefore they are not valid. On the other hand u_1 is selecting the Majorana zero modes that are bonded to the core of vortex.

Now let us look at a little bit more closely to the phase with trivial topology. One would expect not to observe any Majorana zero modes when chemical potential is negative. We should

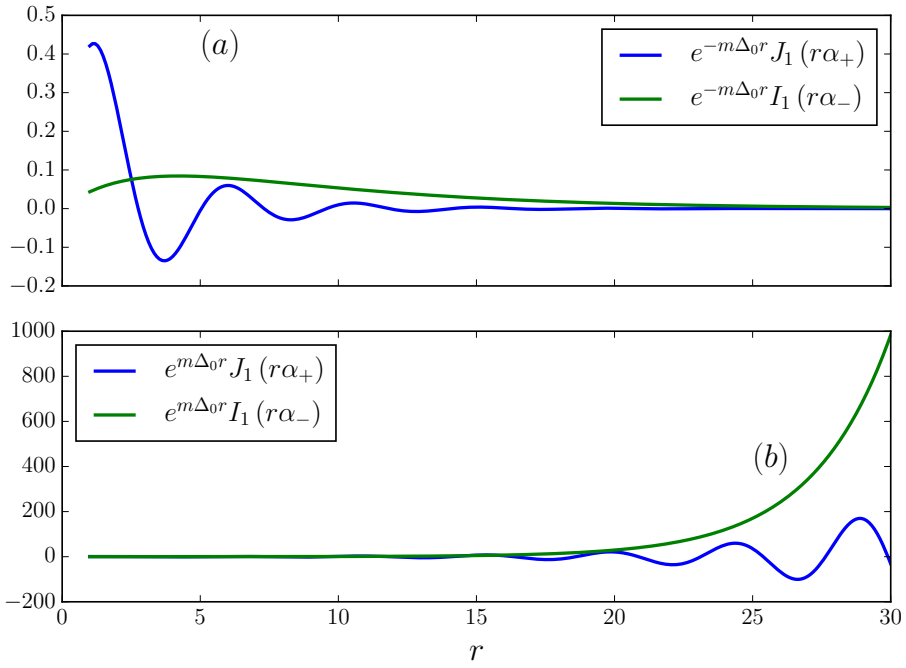

Figure 2.3: The well-behaved solutions to BdG equation at origin are plotted with parameters $m = .5$, $\Delta = .5$ and two different value for chemical potential in order to respect the condition set by the analytic results. For α_+ chemical potential is chosen to be $\mu = .5$ and $\mu = .05$ for α_-. (a) shows that u_1 is bonded to the core of the vortex while (b) reveals that functions associated to solution u_2 are not normalizable.

examine the behavior of u_1 for $\mu < 0$ and see if we can observe any normalizable wavefunction. The asymptotic behavior of u_1 at large radii can be written as

$$u_1(r) \sim e^{(\alpha_- - m\Delta_0)r} \tag{2.30}$$

In the case of $\mu < 0$, α is greater than $m\Delta_0$ which makes $u_1(r)$ to go to infinity as $r \to \infty$ therefore there is no valid solution for trivial topological region.

2.4 Numerical results for Majorana zero modes in $p + ip$ superconductor on an annulus

In order to numerically solve the BdG equation and search for Majorana zero modes, one by discritizing the BdG Hamiltonian in the real space (Eq. 2.16) can write[22]

$$H = \sum_i (4t - \mu)\psi_i^\dagger \psi_i \; - t \sum_{\langle i,j \rangle} \psi_i^\dagger \psi_j - \frac{1}{2} \sum_{\langle i,j \rangle} \left(\Delta_{ij} \psi_i^\dagger \psi_j^\dagger + \text{H.c.} \right) \tag{2.31}$$

with

$$t = \frac{1}{2ma^2} \qquad\qquad \Delta_{ij} = \frac{1}{2}\, \Delta_0\, \chi_{ij}\, e^{i\theta_{i \leftrightarrow j}} \tag{2.32}$$

$$\chi_{ij} = \pm\, \delta_{j, i \pm \hat{x}} \pm i \delta_{j, i \pm \hat{y}} \qquad\qquad \theta_{i \leftrightarrow j} = \frac{1}{2}\,(\theta_i + \theta_j) \tag{2.33}$$

where a is the lattice constant, t is the unit of energy and χ_{ij} is the chirality factor that implement the $p + ip$ pairing. For the discretized Hamiltonian, the bulk energy can be written as

$$E_{\text{bulk}}(\mathbf{k}) = \pm \sqrt{\epsilon(\mathbf{k})^2 + \Delta_0^2 \left[\sin^2(k_x) + \sin^2(k_y) \right]} \tag{2.34}$$

with

$$\epsilon(\mathbf{k}) = 4t - \mu - 2t \left[\cos(k_x) + \cos(k_y) \right]. \tag{2.35}$$

The energy spectrum has gapless points at $\mu = 0, 4t, 8t$. One can show that only $0 < \mu < 4t$ and $4t < \mu < 8t$ would show topologically non-trivial phase and therefore they are the subject to search for Majorana zero modes. Moreover we can show that the mapping

$$\mu \to 8t - \mu \qquad , \qquad \psi_n \to e^{in\pi}\, \psi_n \tag{2.36}$$

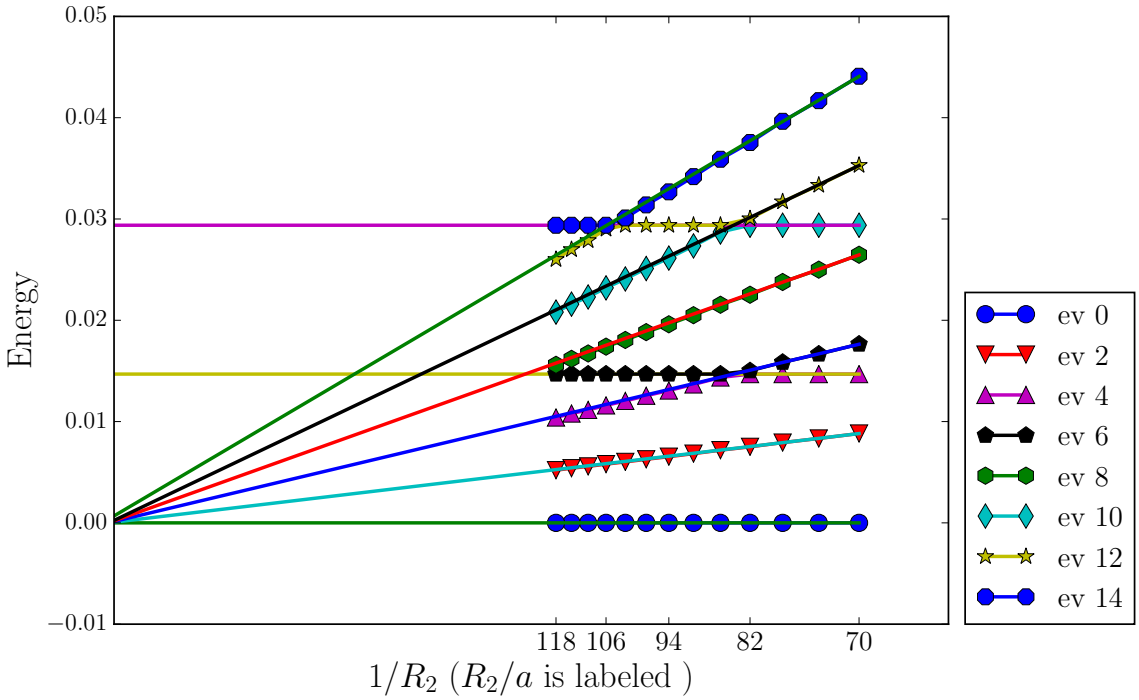

Figure 2.4: The behavior of energy spectrum as a function of system size is plotted. The system contains a $p+ip$ superconductor on an annulus with presence of a vortex at its origin. The chemical potential is chosen so that the system exhibit a non-trivial topological phase. Here used $\mu/t = 2$, $\Delta_0/(at) = 1$, $R_1/a = 40$ and R_2 is the outer radius of the annulus.

would transform each of these two region to another one while keeping the spectrum intact ($H \to -H$) therefore we only consider $0 < \mu < 4t$ in our numerical studies.

The geometry we use here is an annulus with inner and outer radii of R_1 and R_2 respectively. In Fig 2.4 we plotted the energy spectrum of the system while we only kept the positive energies since the particle-hole symmetry can relate each of them to their counterpart with negative energy. Here there are two types of modes, first the one whose energies remains constant as system size increases. These are the modes which are localized around the inner edge of the system. These

modes are normalizable in thermodynamic limit ($R_2 \to \infty$) and are bonded to the core of the vortices. Second, the modes which their energies are decreasing linearly with $1/R_2$. These modes are the ones which are located around the outer ring and are not normalizable in the thermodynamic limit.

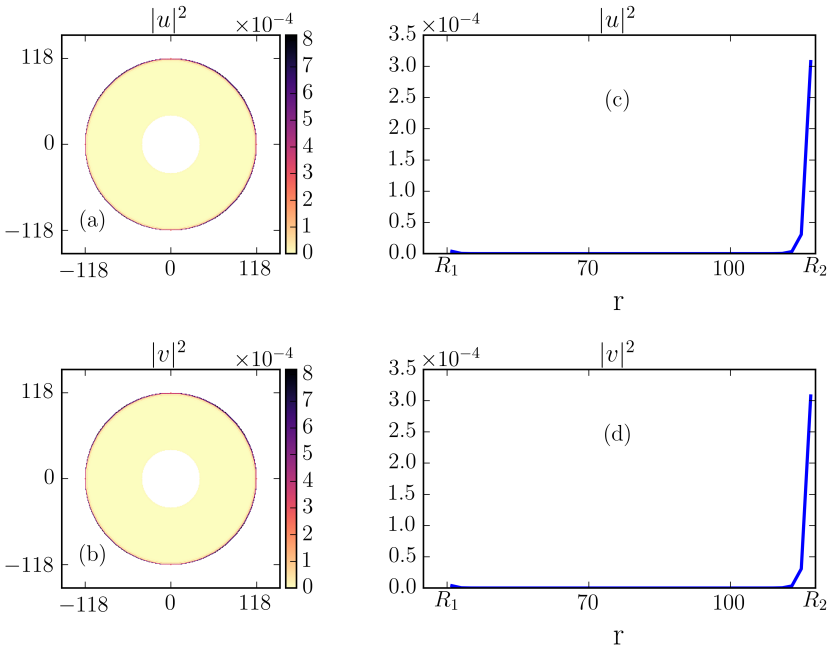

Figure 2.5: The numerical result for one of Majorana zero modes which is localized around the outer ring of annulus has been plotted. . (a) and (b) display the the square of the absolute value of u and v respectively while In (c) and (d) we plotted the radial dependency of those mentioned functions. The parameters are $\mu/t = 2$, $\Delta_0/(at) = 1$, $R_1/a = 40$ and $R_2 = 118$.

Numerically we would find two distinct Majorana zero modes (two orthogonal state with energy of zero), one of which is localized around the inner radius while the other one is located at the outer edge. In Fig 2.5 and Fig 2.6 we plotted square of the absolute value of these eigenfunctions

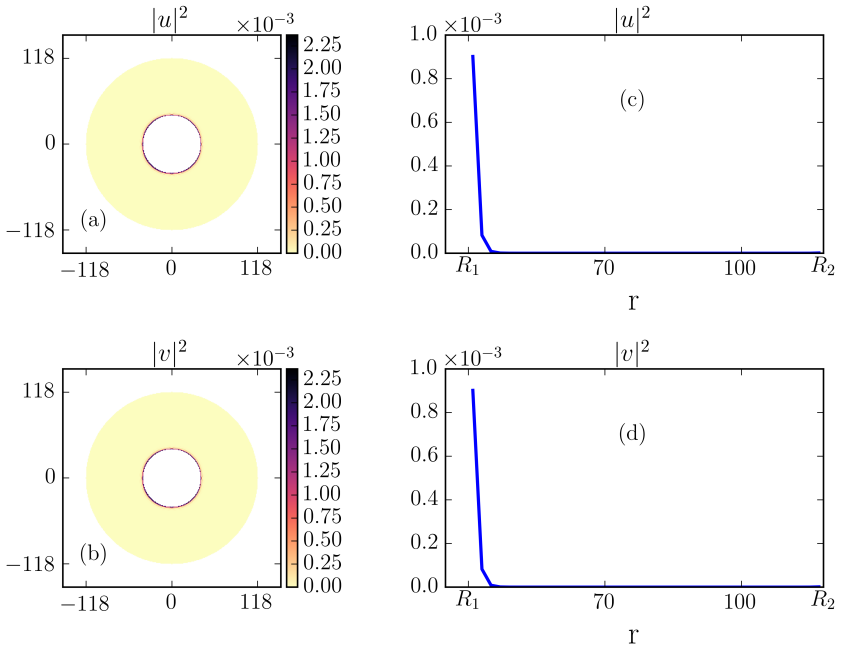

Figure 2.6: The numerical result shows that another one of Majorana zero modes is localized around the inner ring of annulus. . (a) and (b) display the the square of the absolute value of u and v respectively while In (c) and (d) we plotted the radial dependency of those mentioned functions. We used the parameters $\mu/t = 2$, $\Delta_0/(at) = 1$, $R_1/a = 40$ and $R_2 = 118$.

on the annulus also since the we plot them as a function of radius.

2.5 Spinful p-wave superconductors and half quantum vortices

Addition of spin make the problem subtle while much more interesting. Order parameter can be written as a 2×2 matrix to support spin degrees of freedom. Formally, one can write the order parameter for triplet spin paring as

$$\Delta_{\alpha\beta}(\mathbf{k}) = \mathbf{d}(\mathbf{k}) \cdot (\boldsymbol{\sigma} i\sigma_y)_{\alpha\beta} \tag{2.37}$$

where $\sigma_i (i = x, y, z)$ are Pauli matrices and vector $\mathbf{d}(\mathbf{k})$ determines the spin texture. Pauli exclusion principle dictate $\mathbf{d}(\mathbf{k})$ to be an odd function of $\mathbf{k}$. Explicitly for $p + ip$ superconductor one can write[23]

$$\Delta(\mathbf{k}) = \Delta_0 e^{i\phi} \begin{pmatrix} -\hat{d}_x + i\hat{d}_y & \hat{d}_z \\ \hat{d}_z & \hat{d}_x + i\hat{d}_y \end{pmatrix} (k_x + ik_y) \tag{2.38}$$

where Δ_0 is the magnitude of the paring, ϕ is the phase of the superconductor and $\hat{d}$ is the unit vector on which the projection of Cooper pair spin is zero. introducing spin would make the excitation spectrum to be two-fold degenerate ($E_{k,\uparrow} = E_{k,\downarrow}$)

For triplet equal spin pairing, $\hat{d}$ is in $\hat{z}$ direction and to include the vortex we can use the polar angle as the superconducting phase.

$$\Delta(\mathbf{k}) = \Delta_0 e^{i\theta} \begin{pmatrix} 0 & 1 \\ 1 & 0 \end{pmatrix} (k_x + ik_y) \tag{2.39}$$

By looking for Majorana zero modes one can show that there are two orthogonal modes that are bonded to the core of vortices which would make them unstable for observation[24] (any perturbation like Zeeman splitting or spin-orbit interaction would destroy the Majorana zero mode in full quantum vortices). half quantum was introduced to stabilize Majorana zero modes. In the half quantum vortices , phase of superconducting order parameter winds by π(instead of 2π) around the vortex core. For a half quantum vortex to exist, the vector $\hat{d}$ must be able to rotate to ensure the single-valuedness of order parameter. The Order parameter would map to itself under change of sign of vector $\hat{d}$ and shift of the phase ϕ by $\pi : (\phi, \hat{d}) \mapsto (\phi + \pi, -\hat{d})$. The simplest half quantum vortex

can be written as

$$\phi = \theta/2, \qquad \hat{d} = \cos(\theta/2)\hat{x} + \sin(\theta/2)\hat{y} \quad . \tag{2.40}$$

these parameters would simplify the order parameter as

$$\Delta = \Delta_0 \begin{pmatrix} -1 & 0 \\ 0 & e^{i\theta} \end{pmatrix} (k_x + ik_y) \tag{2.41}$$

which shows only one full vortex in the down spin and no vortex in the up spin. Consequently in this configuration only one Majorana zero mode can be observed for each boundaries of the topological region.

Although, Majorana zero modes in the systems exhibiting half quantum vortices are stable to any local perturbation (including spin orbit interaction and Zeeman splitting), isolated half quantum vortices have not been seen in the bulk material. In the next chapter we talk about the possible reasoning why they have not been observe and how to overcome them.

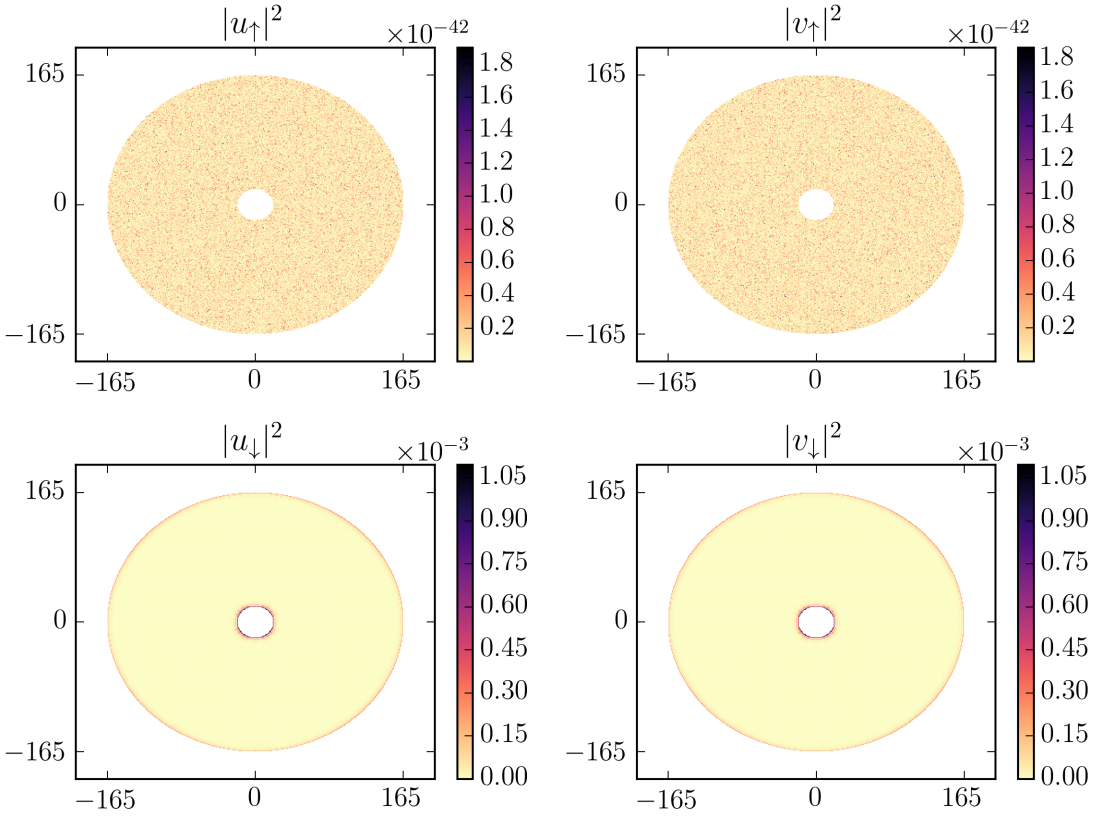

Figure 2.7: A system supporting half quantum vortex exhibit only one Majorana zero mode for each boundaries of the system. One can see that only down spin here display the Majorana zero modes on the boundaries. For the numerical calculation we used $\Delta_0/(at) = .5$, $\mu/t = 2$, $R_1/a = 20$ and $R_2/a = 165$

Chapter 3

Majorana zero modes in p+ip superconducting rings with half quantum flux in the presence of d-solitons

As we mentioned in the chapter 2, isolated half quantum vortices have not been observed in the bulk material. One of the reasons can be that the spin current unlike the normal suppercurrent does not screened at large distances and that would increase the energy of a half quantum vortex compare to a full quantum vortex. One using a mesoscopic rings can put a cutoff on the logarithmic term in energy due to spin current and resolve the problem.

The other problem for observing half quantum vortices is presence of the spin orbit interaction.[25] In reality any material has non-zero spin orbit coupling that would contribute to the

energy

$$E_{\text{so}} = -\lambda_{\text{so}}(\hat{d} \cdot \hat{l})^2 \tag{3.1}$$

Where λ_{so} is spin orbit coupling, $\hat{d}$ is the spin texture and $\hat{l}$ is a preferred direction in the orbital space giving the direction of the Cooper pair angular momentum. For $p + ip$ pairing $\hat{l}$ is in $\hat{z}$ direction and for a half quantum vortex $\hat{d}$ lies in $x - y$ plane which shows that the E_{so} is at its maximum ($E_{\text{so}} = 0$).

A Model has been proposed by Kee and Sigrist[13] to show that half quantum vortex can have lower energy than a full quantum vortex in presence of in plain magnetic field and non-zero spin orbit coupling.

3.1 The Model

In General the BdG Hamiltonian in Nambu-spinor notation in momentum space can be written as

$$H_{\text{BdG}} = \frac{1}{2} \begin{pmatrix} \epsilon(\mathbf{k})\sigma_0 & \Delta(\mathbf{k}) \\ \Delta^\dagger(\mathbf{k}) & -\epsilon^*(\mathbf{k})\sigma_0 \end{pmatrix} \tag{3.2}$$

where

$$\epsilon(\mathbf{k}) = \left(\hbar^2 k^2/2m - \mu\right) \tag{3.3}$$

is the single particle kinetic energy, μ is the chemical potential, m is mass and for $p + ip$ superconductors $\Delta(\mathbf{k})$ is define in Eqs. (4.8) and (4.9) while $\hat{d}$ and ϕ are given by

$$\hat{d} = \hat{z}\cos(\alpha_\theta) + \hat{\theta}\sin(\alpha_\theta)$$

$$\phi = -4\, s_r \arctan[e^{\theta/l}] + (s_r + \frac{1}{2}) \times (\theta + \pi) \tag{3.4}$$

with

$$\alpha_\theta = 2\arctan\left[e^{\theta/l}\right] \tag{3.5}$$

$$l = \sqrt{\frac{K}{\lambda_{\text{so}} R_{\text{in}}^2}\left(1 - 4s_r^2\right)} \tag{3.6}$$

where $-\pi < \theta < \pi$ is the polar angle, s_r is the radial component of the in-plane spin magnetization, K is the stiffness, R_{in} is the inner radius of the annulus and λ_{so} is spin-orbit coupling.

In this model in order to guarantee the single-valuedness of order parameter l has to be small, $l \ll \pi$, therefore α and ϕ are bounded between 0 and π. By this formulation α_θ varies such that around $\theta = 0$ the d-vector changes from $\hat{z}$ to $-\hat{z}$ this is a d-soliton centered around $\theta = 0$ (see Fig. 3.1). This would result in having a half quantum vortex.

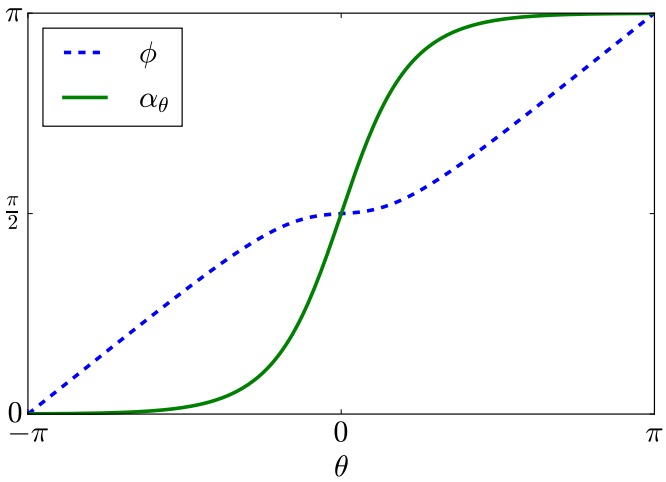

Figure 3.1: The behavior of α_θ and ϕ are shown as a function of θ. For illustration we took $\lambda_{\text{so}} R_{\text{in}}^2 = 5K$ and $s_r = 1/8$. The d-soliton is centered around $\theta = 0$

The bulk excitation energies are given by

$$E_{\text{bulk}}(\mathbf{k}) = \pm\frac{1}{2}\sqrt{\epsilon(\mathbf{k})^2 + \Delta_0^2 k^2} \tag{3.7}$$

This equation shows that the bulk energy spectrum is gapped and for $\mu > m\Delta_0^2/\hbar^2$ the gap would be given by $E_{\text{Gap}} = \Delta_0 k_F$. For positive μ the system is in a topological parameter region.

3.2 The Solution

In this section we will use numerical calculation to find the energy spectrum and the behavior of the ground state in this model. The goal is to show that the energy of Majorana zero mode would go to zero exponentially as a function of system size. In order to solve this problem numerically one should write the BdG Hamiltonian in the real space discretizwe and diagonalized the Hamiltonian. The BdG Hamiltonian in the real space can be written as

$$H_{\text{BdG}} = \frac{1}{2}\begin{pmatrix} (-t\nabla^2 - \mu)\sigma_0 & -i\Delta(\mathbf{r})\left(\partial_x + i\partial_y\right) \\ -i\Delta^*(\mathbf{r})\left(\partial_x - i\partial_y\right) & -(-t\nabla^2 - \mu)\sigma_0 \end{pmatrix} \tag{3.8}$$

where $t = \frac{\hbar^2}{2m}$ is the hopping parameter and $\Delta(\mathbf{r})$ is a 2×2 matrix

$$\Delta_{\alpha\beta}(\mathbf{r}) = \Delta_0 e^{i\phi}\hat{d}\cdot\left(\boldsymbol{\sigma} i\sigma_y\right)_{\alpha\beta} \tag{3.9}$$

where ϕ and $\hat{d}$ are defied in Eq. 4.11

By discretizing the BdG equations we can exactly diagonalize the Hamiltonian and look for the lowest energies.

$$\begin{aligned} H = &\sum_{i,\sigma}(4t-\mu)\psi^\dagger_{i,\sigma}\psi_{i,\sigma} \; - t\sum_{\langle i,j\rangle}\psi^\dagger_{i,\sigma}\psi_{j,\sigma} + \\ &\frac{1}{2}\sum_{\langle i,j\rangle\sigma\sigma'}\Delta^{\sigma\sigma'}_{ij}\psi^\dagger_{i,\sigma}\psi^\dagger_{j,\sigma'} + \text{H.c.} \end{aligned} \tag{3.10}$$

where

$$\Delta_{ij}^{\alpha\beta} = \frac{1}{2}\chi_{ij}\Delta_{\alpha\beta} \tag{3.11}$$

$$\chi_{ij} = \mp i\ \delta_{j,i\pm\hat{x}} \pm \delta_{j,i\pm\hat{y}} \tag{3.12}$$

where χ_{ij} is taking care of the $p + ip$ chirality. After discretizing the dispersion of bulk energy can be reduced to

$$\epsilon(\mathbf{k}) = 4t - \mu - 2t\left[\cos(k_x) + \cos(k_y)\right] \tag{3.13}$$

$$E_{\text{bulk}}(\mathbf{k}) = \pm\frac{1}{2}\sqrt{\epsilon(\mathbf{k})^2 + \Delta_0^2\left[\sin^2(k_x) + \sin^2(k_y)\right]} \tag{3.14}$$

The spectrum has gapless points for $\mu = 0, 4t, 8t$. Therefore one can show that the system is in topological phase for $0 < \mu < 4t$ or $4t < \mu < 8t$. Since by shifting chemical potential $\mu \to 8t - \mu$ and a unitary transformation $\psi_{n,\sigma} \to e^{in\pi}\psi_{n,\sigma}$ Hamiltonian would take a negative sign $H \to -H$, there is a mapping between these two topological regions and therefore we can focus our attention attentions only on the region $0 < \mu < 4t$. Moreover, in order to make sure magnitude of order parameter ,Δ_0, keeps its physical meaning, i.e. bulk gap being proportional to magnitude of order parameter ,$E_{\text{Gap}} \sim \Delta_0$ the chemical potential is restricted to

$$\frac{\Delta_0^2}{2t} < \mu < 4t - \frac{\Delta_0^2}{2t} \tag{3.15}$$

In this limits one can show the bulk gap is given by

$$E_{\text{Gap}} = \Delta_0\sqrt{\frac{\mu}{t} - \frac{\mu^2}{4t^2}} \tag{3.16}$$

Using exact diagonalization one can find the energy spectrum of the well localized modes on a annulus. Our investigation shows that there is one Majorana zero mode for each boundary

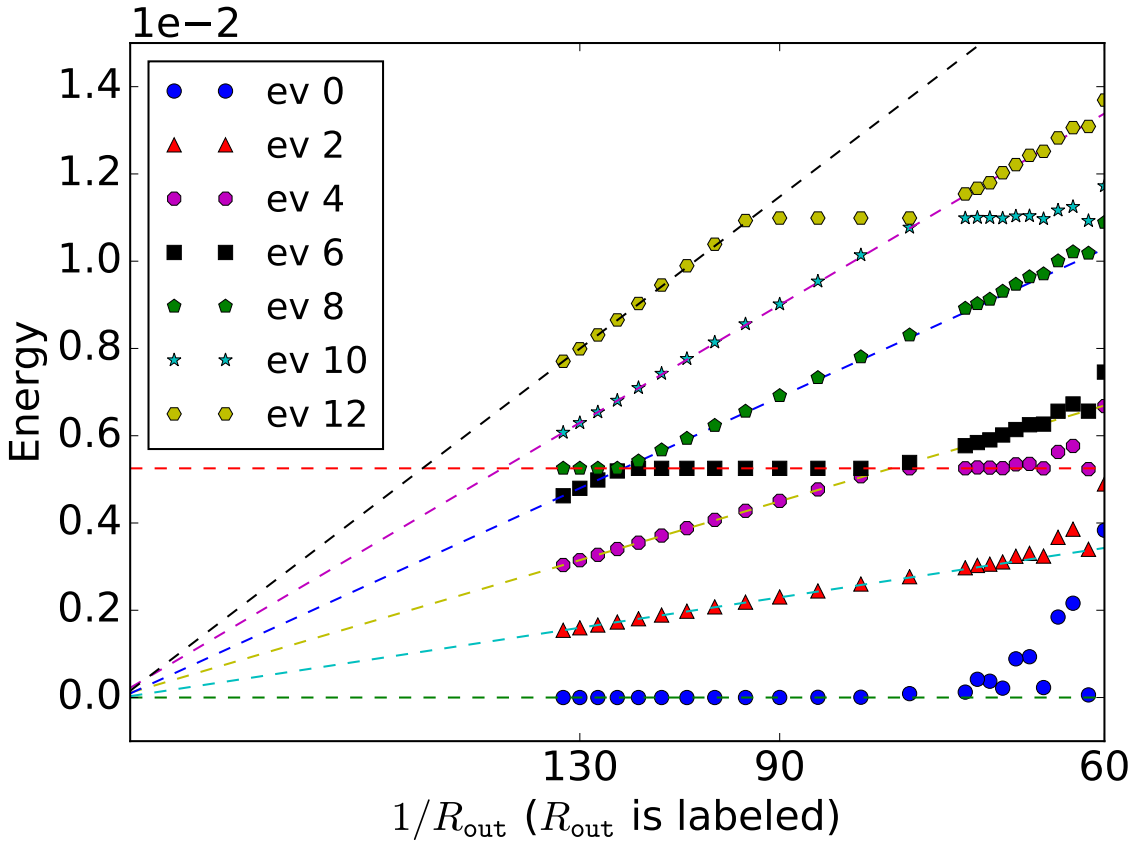

Figure 3.2: The energy spectrum for localized modes as a function of inverse of the outer radius $1/R_{\text{out}}$. Here we took $\mu/t = 2$, $\Delta_0/t = 0.5$ and $R_{\text{in}} = 40$

of the system. As shown in the Fig. 3.2 there are two degenerate zero modes due to particle-hole symmetry which are localized on inner and outer rings of the system. The modes with energies that goes to zero linearly as a function of inverse of outer radius, i. e. $1/R_{\text{out}}$, are localized on the outer edge and are not normalizable in the thermodynamic limit. On the other hand the modes that are localized on the inner radius of the system have constant energies as we increase the size of the system.

In the simplest half quantum vortex on an annulus, the energy of the inner-edge modes are

quantized as $E_{\text{vortex}} \sim n\Delta_0/R_{\text{in}}$ where n is an integer and R_{in} is the inner radius of the annulus.[1] By generalizing the result, one can show that for the Majorana modes localized at the inner annulus edge, the energy spectrum can be simplified as

$$E_{\text{in}} = n\omega, \qquad \omega = \frac{\Delta_0}{R_{\text{in}}}\sqrt{1 - \frac{\mu}{4t}} \tag{3.17}$$

which was confirmed numerically.

Chapter 4

Energy splitting of two Majorana zero modes in finite size systems

It has been shown that Majorana zero modes can display energy splitting due to intra-vortex tunneling in $p + ip$ superconductors. By preparing two vortices and looking at the energy splitting behavior as a function of distance between them, one would observe an oscillation on top of exponentially decaying function.[26]

In this chapter our goal is to find the energy splitting of Majorana zero modes in finite size systems due to small but non-zero overlap between them. Let us prepare a system on an annulus whose chemical potential is positive (topological) in the middle and negative elsewhere (see Fig. 4.1).

$$\mu(r) = \begin{cases} \mu_{\text{out}} & r < R_1 \\ \mu_{\text{in}} & R_1 \leq r \leq R_2 \\ \mu_{\text{out}} & r > R_2 \end{cases} \tag{4.1}$$

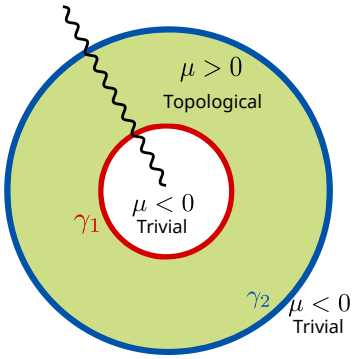

Figure 4.1: The shaded region represent a positive (topological) chemical potential on an annulus. The presence of a vortex at the origin forces a branch cut which is represented as a wavy line while γ_1 and γ_2 illustrate the expected location of Majorana zero modes.

of a place where where $\mu_{\text{in}} > 0$ and $\mu_{\text{out}} < 0$.

First we numerically solve this problem to find both energy spectrum and ground state wavefunctions ($|GS\rangle$). In order to make unitless quantities, in our numerical calculations we take t and a to be unit of energy and length respectively. In Fig. 4.2 we plotted the two components of ground state in Nambu spinor notation ($|GS\rangle = (u, v)^T$). We also plotted u as a function of width of annulus (see Fig. 4.3) which would exhibit the fact that Majorana modes are localized around each boundaries of the system (R_1 and R_2). Now we can cook up two wavefunctions with approximately zero energy expectation values with similar properties to Majorana modes. Therefore each function should be approximately zero, around one of the edges, whereas they remain non-zero around the other edge. Notice that these functions are not eigenfunctions of Hamiltonian and consequently they would have non-zero crossing term i.e. $\langle\psi_2|H|\psi_1\rangle$ which would give rise to the energy splitting between them.

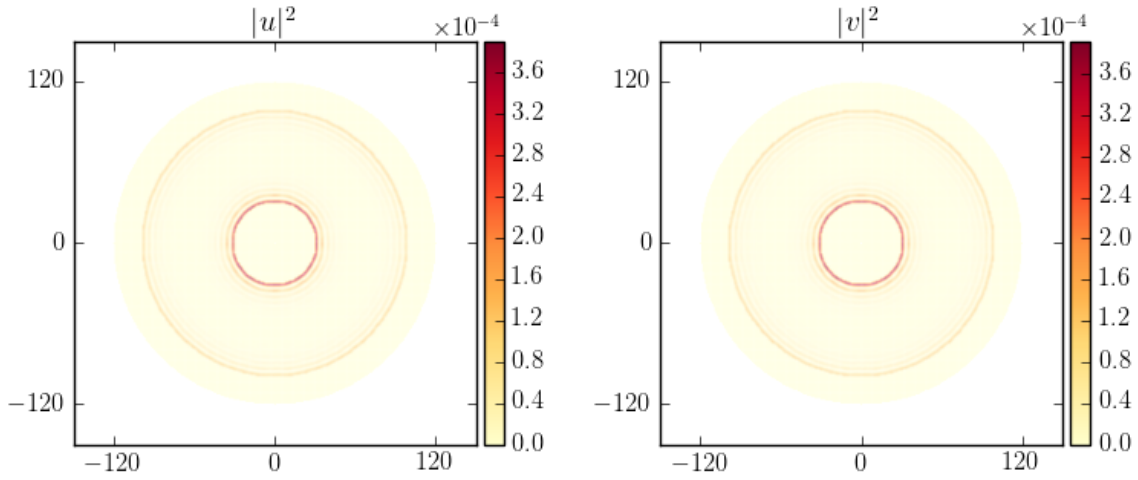

Figure 4.2: Plot of the numerical results for the ground state of a system with $\mu_{\text{in}}/t = 0.5$, $\mu_{\text{out}}/t = 100$, $\Delta_0/(ta) = 0.2$, $R_1/a = 30$ and $R_2/a = 100$. u and v are the two component of spinor $|GS\rangle$

Since we would want the expectation energy to be approximately zero we will use the solutions we got section 2.3. First we start by writing the wavefunction that would be maximized around the inner ring of the annulus i.e. ψ_1.

which is monotonically increasing from origin to the inner ring(R_1) of the sample and exponentially decreasing in radii that are greater than R_1.

$$\psi_1 = e^{-m\Delta_0 r} \begin{cases} c_1 I_1\left(r\alpha_{\text{out}}\right) & r < R_1 \\ c_2 J_1\left(r\alpha_{\text{in}}\right) + c_3 Y_1\left(r\alpha_{\text{in}}\right) & r > R_1 \end{cases} \tag{4.2}$$

with

$$\alpha_{\text{in}} = \sqrt{2m\mu_{\text{in}} - m^2\Delta_0^2}$$

$$\alpha_{\text{out}} = \sqrt{m^2\Delta_0^2 - 2m\mu_{\text{out}}}$$

where c_1, c_2 and c_3 are constants and will be fixed by normalization and boundary conditions at R_1.

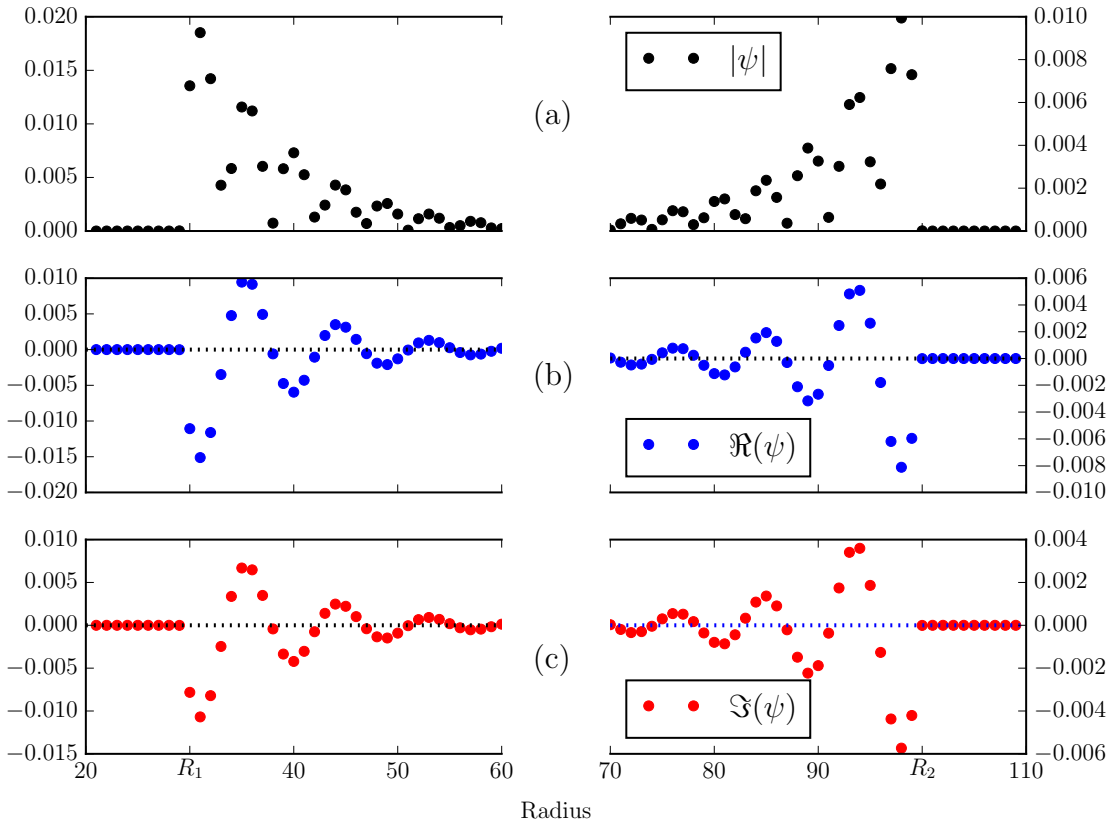

Figure 4.3: Radial dependency of ground state ($|GS\rangle$) with $\mu_{\text{in}}/t = 0.5$, $\mu_{\text{out}}/t = 100$, $\Delta_0/(ta) = 0.2$, $R_1/a = 30$ and $R_2/a = 100$. (a) is the plot of absolute value of the ground state while (b) and (c) are the real part and imaginary part of ground state respectively.

This wavefunction is monotonically increasing as we approach the inner ring and would exponentially decays afterwards. Since all of our boundaries are far from origin we can use the asymptomatic behavior of Bessel functions.

$$
\begin{aligned}
J_1(z) &\sim \sqrt{\frac{2}{\pi z}}\left(\cos(z-\frac{3\pi}{4})\right) \\
Y_1(z) &\sim \sqrt{\frac{2}{\pi z}}\left(\sin(z-\frac{3\pi}{4})\right) \\
I_1(z) &\sim \frac{1}{\sqrt{2\pi z}}\, e^{z} \\
K_1(z) &\sim \sqrt{\frac{\pi}{2z}}\, e^{-z}
\end{aligned}
$$

Now we will find the expectation value of the Hamiltonian, i.e. $\langle\psi_1|H|\psi_1\rangle$. Since we used the exact solution for zero energy for radii less that R_2, we only need to compute the expectation outside of the annulus. Also, because we are only changing chemical potential at the boundary, the differential equation 2.27 would tell us that ψ_1 is an eigenfunction of H in the outside region. The expectation value would simplify to

$$\langle\psi_1|H|\psi_1\rangle = (\mu_{\text{in}} - \mu_{\text{out}}) \int_{R_2}^{\infty} r\, |\psi_1(r)|^2\, dr \sim e^{-2(R_2-R_1)/\xi} \tag{4.3}$$

where $\xi = \frac{1}{m\Delta_0}$. Since we are working in the limit of $(R_2 - R_1) \gg \xi$, we only would keep up to first order in $e^{-(R_2-R_1)/\xi}$ and therefore we would neglect this term.

Next we will use the solution for u_2 (Eq. 2.29) to write another solution which would be localized around R_2.

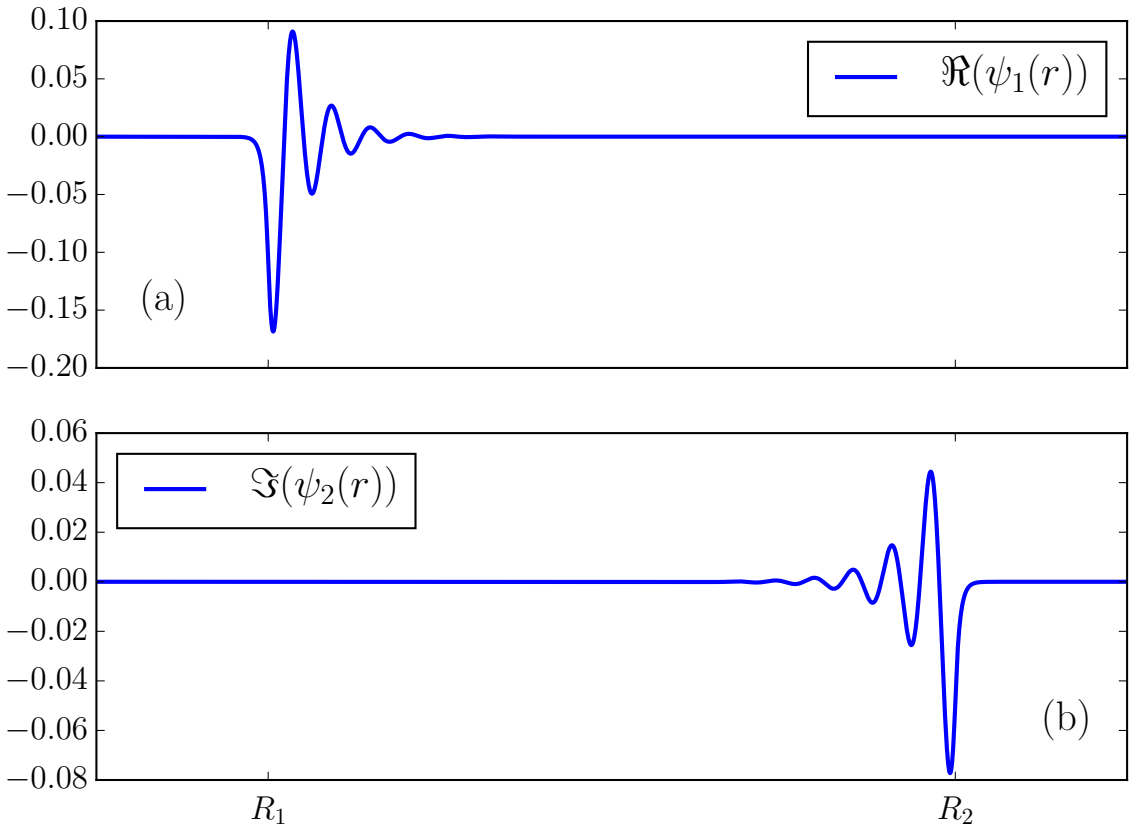

Figure 4.4: Illustration of the wavefunctions ψ_1 and ψ_2 after normalization and matching boundary conditions. Since ψ_1 is real and ψ_2 is pure imaginary, the real and imaginary part are plotted respectively in (a) and (b).

$$\psi_2 = ie^{+m\Delta_0 r} \begin{cases} \tilde{c_1} J_1\left(r\alpha_{\text{in}}\right) + \tilde{c_2} Y_1\left(r\alpha_{\text{in}}\right) & r < R_2 \\ \\ \tilde{c_3} K_1\left(r\alpha_{\text{out}}\right) & r > R_2 \end{cases} \tag{4.4}$$

Here $\tilde{c_1}$, $\tilde{c_2}$ and $\tilde{c_3}$ are constants and will be fixed by boundary conditions at R_2 and normalization of the wavefunction. Although this wavefunction is not well-behaved at the origin, but this should not worry us due to presence of vortex at the origin which has a non-zero core radius. Energy expectation value can be written as

its behavior near the origin.

$$\langle\psi_2|H|\psi_2\rangle = (\mu_{\text{in}} - \mu_{\text{out}}) \int_{\xi}^{R_1} r\, |\psi_2(r)|^2\, dr \sim e^{-2(R_2 - R_1)/\xi} \tag{4.5}$$

which again will be neglected.

In order to calculate the energy we need to find the crossing term between these two solution.

$$\Delta E = 2\, i\, \langle\psi_2|H|\psi_1\rangle = 2\, i\, (\mu_{\text{in}} - \mu_{\text{out}}) \int_{R_2}^{\infty} r\, \psi_2(r)^*\, \psi_1(r)\, dr$$

$$= -\frac{8\, m\, \Delta_0\, \mu_{\text{in}}\, \left(\Delta_0 m - \alpha_{\text{out}}\right)\, e^{-m\Delta_0(R_2 - R_1)} \sin\left[(R_2 - R_1)\, \alpha_{\text{in}} + \phi_0\right]}{\left(\Delta_0 m + \alpha_{\text{out}}\right) \alpha_{\text{in}}} \tag{4.6}$$

where

$$\phi_0 = \arctan\left(\frac{2\alpha_{\text{in}}\alpha_{\text{out}}}{\alpha_{\text{out}}^2 - \alpha_{\text{in}}^2}\right)$$

Now we can take the limit of $\mu_{\text{out}} \to -\infty$ which would simplify the energy splitting to

$$\Delta E = \frac{8\, m\, \Delta_0\, \mu_{\text{in}}\, e^{-m\Delta_0(R_2 - R_1)} \sin\left[(R_2 - R_1)\, \alpha_{\text{in}}\right]}{\alpha_{\text{in}}} \tag{4.7}$$

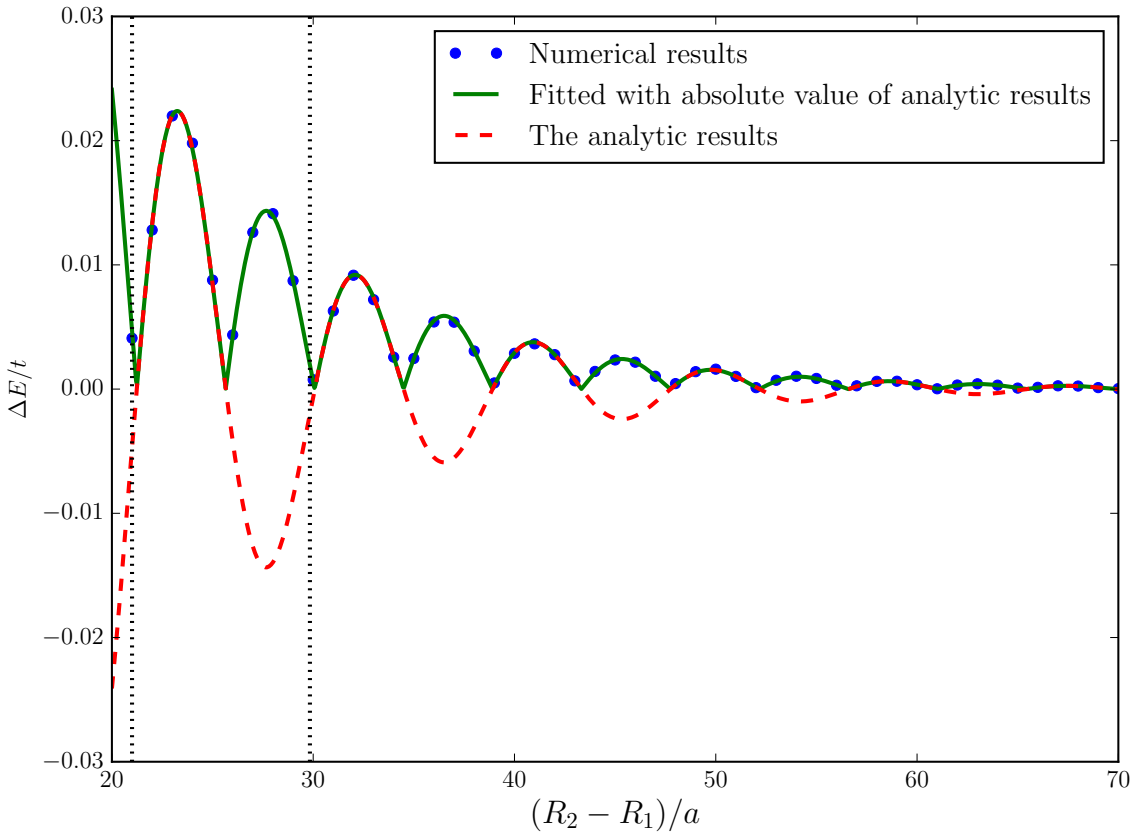

Figure 4.5: Energy splitting of two Majorana modes as a function of width of annulus($R_2 - R_1$). Here we take $\mu_{\text{in}}/t = 0.5$, $\mu_{\text{out}}/t = 100$ and $\Delta_0/(ta) = 0.2$. The dotted line would display the numerical results of absolute value of splitting while the solid line would show the fitting with absolute value of the analytic result Eq. 4.7 and the dashed line is the analytic result without taking absolute value.

here we can see the energy splitting on top of decaying exponentially has a oscillation as a function of width of annulus ($R_2 - R_1$). The numerical result would fit perfectly with Eq. 4.7 (see Fig. 4.5)

4.1 Energy splitting of two Majorana zero modes in finite size systems in the presence of d-solitons

Let us briefly review what we know about the model presented by Kee and Sigrist to have a half quantum vortex with presence of d-soliton.The superconducting order parameter in this model can be written as

$$\Delta_{\alpha\beta}(\mathbf{k}) = \mathbf{d}(\mathbf{k}) \cdot (\boldsymbol{\sigma} i\sigma_y)_{\alpha\beta} \tag{4.8}$$

where $\sigma_\mu(\mu = x, y, z)$ are Pauli matrices and here $\mathbf{d}(\mathbf{k})$ can be written as

$$\mathbf{d}(\mathbf{k}) = \Delta_0 e^{i\phi} \hat{d}(k_x + ik_y) \tag{4.9}$$

where Δ_0 is the magnitude of the order parameter, ϕ is the phase angle and $\hat{d}$ is the unit vector on which the projection of Cooper pair spin is zero.

$$\hat{d} = \hat{z}\cos(\alpha_\theta) + \hat{\theta}\sin(\alpha_\theta) \tag{4.10}$$

$$\phi = -4\, s_r \arctan[e^{\theta/l}] + (s_r + \frac{1}{2}) \times (\theta + \pi) \tag{4.11}$$

with

$$\alpha_\theta = 2\arctan[e^{\theta/l}], \qquad l = \sqrt{\frac{K}{\lambda_{\text{so}} R_{\text{in}}^2}(1 - 4s_r^2)} \tag{4.12}$$

where $-\pi < \theta < \pi$ is the polar angle, s_r is the radial component of in-plane spin magnetization, K is the stiffness , R_{in} is the inner radius of the annulus and λ_{so} is spin-orbit coupling. We define a

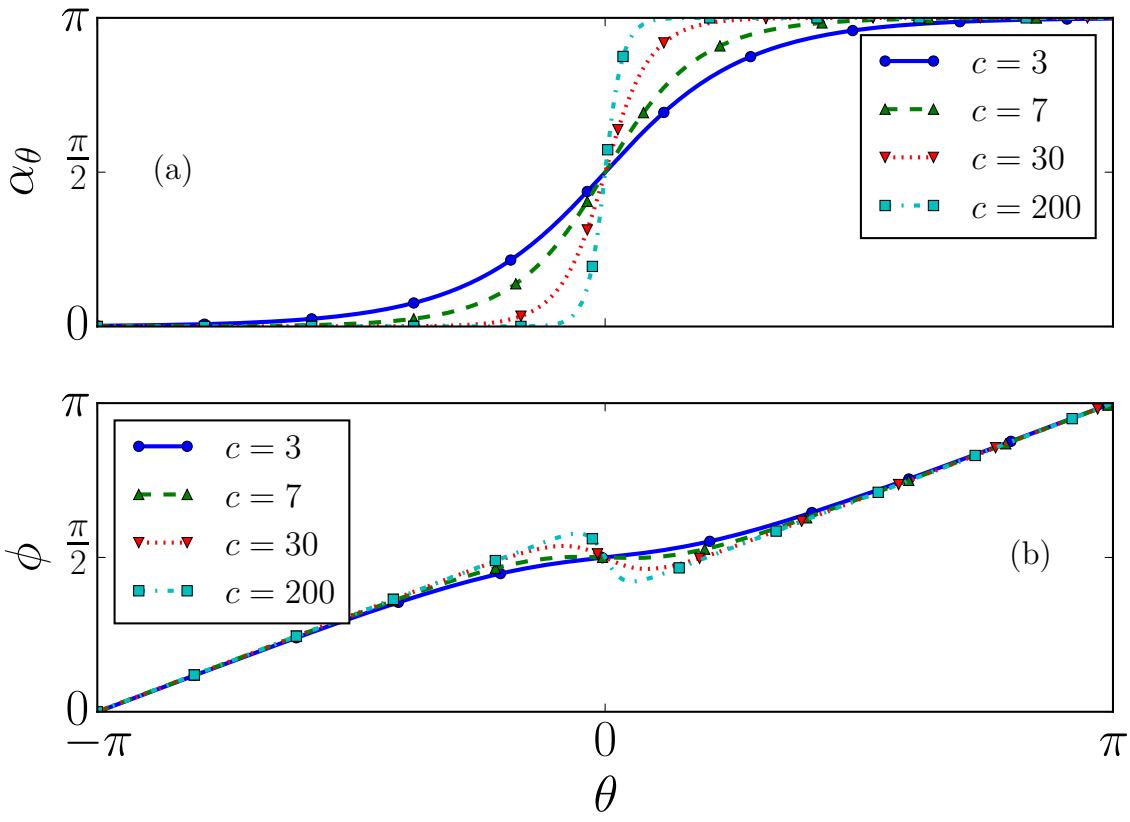

Figure 4.6: (a) α_θ is plotted for different values of c. By increasing c, sharpness in α_θ has, been increased. (b) The Illustration of ϕ as a function of θ. Here s_r (radial magnetization) is taken to be 1/4.

coefficient c that controls the sharpness in α_θ.

$$c = \frac{\lambda_{so} R_{in}^2}{K} \tag{4.13}$$

In Fig. 4.6 α_θ and ϕ are plotted versus θ for different values of c. would change by increasing c.

Our goal in this section is to study the energy splitting of Majorana zero modes and observed that how well they matched with analytic results we got in section 4.1 for a normal half quantum vortex (Eq. 4.7). correspondingly we numerically calculate energy of Majorana zero

modes for different values of c. Using the analytic solution we try to find the best fit within our error of numerical calculation. The setup of the problem is very similar to section 4.1 where the geometry is a annulus which would divide the space to three region. Only middle is a topological region ($\mu > 0$) and other regions have negative chemical potential.

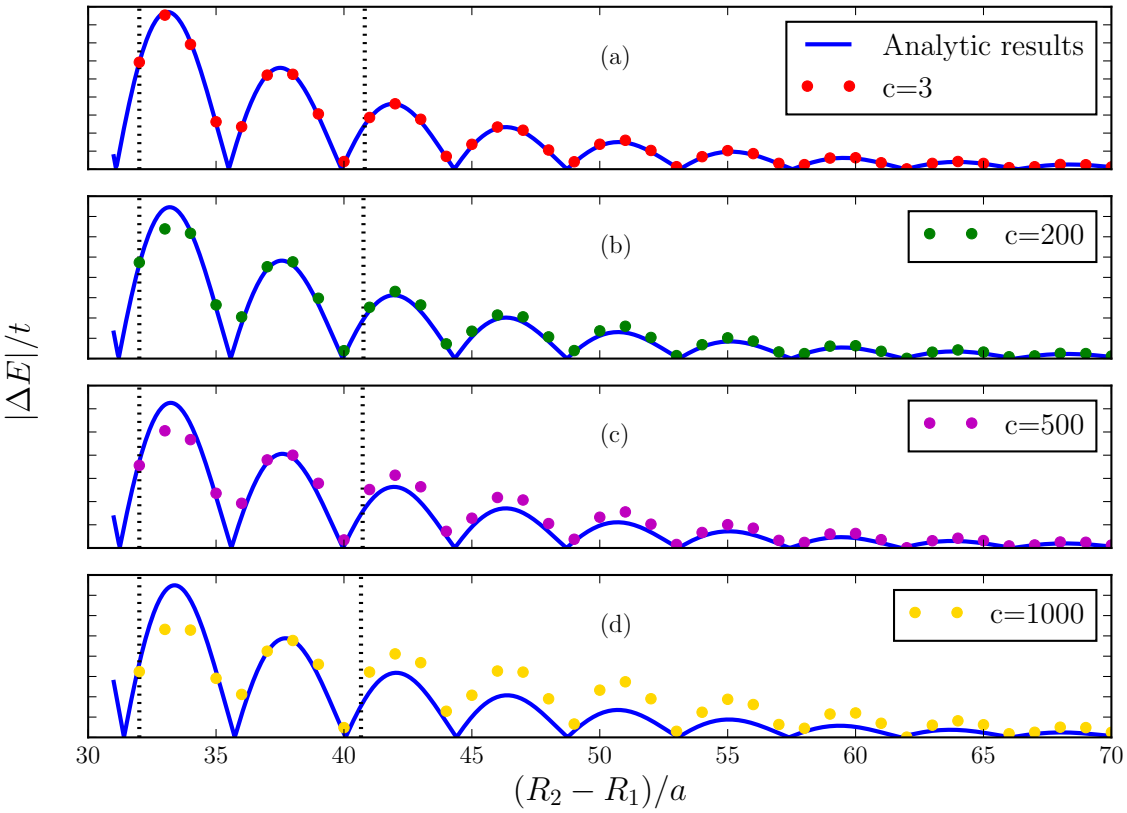

Figure 4.7: Energy splitting of Majorana zero modes in presence of a d-soltion for different values of c, sharpness, has been plotted to show how well the analytic solution would agree with them. We take $\mu_{\text{in}}/t = 0.5$, $\mu_{\text{out}}/t = 100$ and $\Delta_0/(ta) = 0.2$. The dots are the numerical result and the solid(blue) line would show the best fit using analytic expression that has been calculated for a half quantum vortex without having any d-soliton.

Although, for small values of c the analytic solution for half quantum vortex would perfectly describe the system with d-soliton, but as we increase c the analytic result (Eq. 4.7) cannot explain the numerical results very well. In Fig. 4.7 the numerical results of calculation for energy splitting fitted with analytic solution has been plotted.

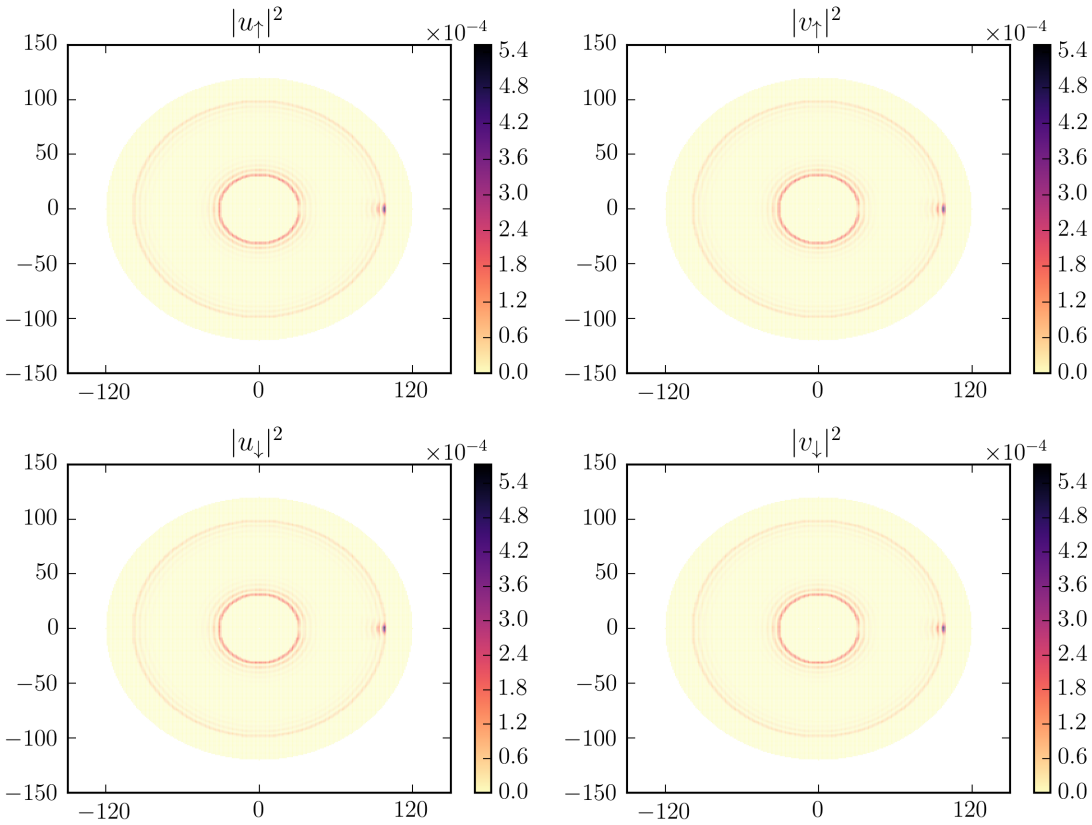

Figure 4.8: Wavefunction of Majorana zero mode in presence of the d-soliton for a large sharpness($c = 1000$). In the numerical calculation we take $R_1/a = 30$, $R_2/a = 100$, $\mu_{\text{in}}/t = 0.5$, $\mu_{\text{out}}/t = 100$ and $\Delta/(ta) = .5$, where a and t are units of length and energy respectively.

It is instructive to look at the wave function of Majorana zero mode in presence of d-soliton for a very large sharpness coefficient (c). Since the system has two spins ($\downarrow$ and $\uparrow$) and due

to particle-hole symmetry, we have four different components for each eigenfunction. In Fig. 4.8 we plotted all four components of the ground state for $c = 1000$. The plot would show that most of the wavefunction on the outer ring (R_2) are concentrated around the d-soliton while in the inner ring the wavefunction is repelled from position of d-soliton

Chapter 5

Array of vortices in the d-wave superconductors

In this chapter we consider an array of vortices in a d-wave superconductor and we search for Majorana zero modes. There are arguments[27–29] supported by index theorem that talk about existence of stable Majorana zero modes when the product of vorticity and the perpendicular component of orbital angular momentum to the plane of superconductor (l_z) is an half odd integer. This argument is definitely true for the case of half quantum vortex in a $p + ip$ superconductor since the the vorticity is a half and the z component of angular momentum is one. The next logical place to check this theory is a d-wave superconductor where orbital angular momentum normal to the plane is two ($l_z = 2$). Consequently, we need one quarter of a quantum vortex to check the theory. While isolated one quarter vortices are not allowed due to single-valuedness of order parameter, we effectively can create one in an array of vortices.

Before we move on to setting up the problem, we need to show that the spectrum of the

d-wave order parameter is fully gapped and also we have to calculate the Chern number to make sure that we are working in a non-trivial phase.

In d-wave superconductor we have singlet paring and therefore the BdG Hamiltonian in nambu notation can be written as

$$H_{\text{BdG}} = \begin{pmatrix} \xi_k & \Delta_{\mathbf{k}} \\ \Delta_{\mathbf{k}}^* & -\xi_k \end{pmatrix} \tag{5.1}$$

where ξ_k is counting for the single particle Hamiltonian, and $\Delta_{\mathbf{k}}$ is the order parameter. The order parameter for $d + id$ superconductor is written as

$$\Delta_{\mathbf{k}} = \Delta_0(k_x^2 - k_y^2 + ik_xk_y) \tag{5.2}$$

where Δ_0 is order parameter magnitude which is constant. One should notice here that the unit of Δ_0 is *energy* $\times$ *Length*^{2}. Hamiltonian (5.1) can be diagonalized using a Bogoliubov transformation to get the energy spectrum

$$E_{\mathbf{k}} = \sqrt{\Delta_0^2\left(k_x^4 + k_y^4 - k_x^2k_y^2\right) + \xi_k^2} \tag{5.3}$$

which shows that the spectrum is fully gapped (see Fig. 5.1)

Using $H_{\text{BdG}}(\mathbf{k}) = \mathbf{h}(\mathbf{k}) \cdot \boldsymbol{\sigma}$ one should be able to construct the unit vector $\hat{\mathbf{h}}(\mathbf{k})$ and map the 2D space of momentum to a unit sphere. For the case of positive chemical potential, $\mu > 0$, we can show that at $k = 0$, the unit vector is pointing toward the south pole and as we go to $k \to \infty$, the unit vector is parallel to $\hat{z}$. Therefore, one can realize that at least this phase would not be topologically trivial. One using Eq. 2.21 can show that the Chern number for this system is 2.

As we promised, we would introduce an array of vortices that effectively can carry one quarter of quantum flux by adding a defect to the system. In Fig. 5.2 one can see a configuration that

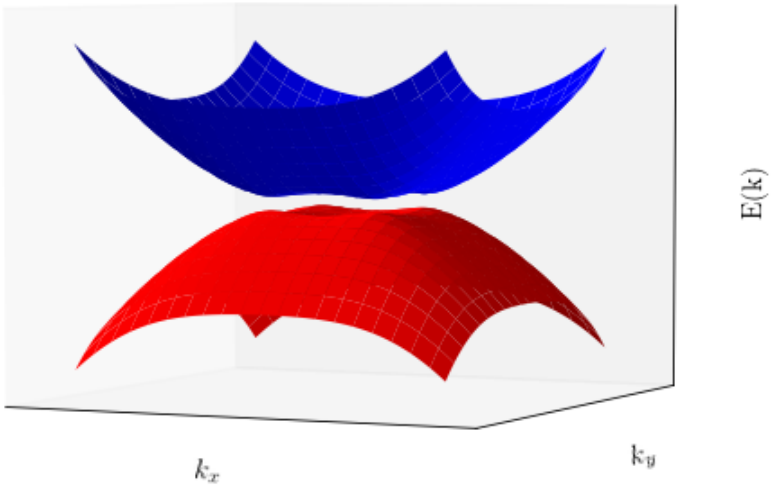

Figure 5.1: The spectrum of the $d+id$ superconductors. One can notice that the spectrum is gapped everywhere.

has a defect in the middle. On each corner of that defect we would expect to observe a Majorana zero mode since the effective vorticity is one quarter.

By writing BdG equations in real space for $d+id$ superconductors and using the order parameter for an array of vortices as

$$\Delta(\mathbf{r}) = \Delta_0 \prod_{j \in \text{Vortices}} e^{i\theta(\mathbf{r}-\mathbf{r_j})} \tag{5.4}$$

where the product runs over all vortices, Δ_0 is the magnitude of order parameter, r_j is the position of the vortex j and $\theta(\mathbf{r}-\mathbf{r_j})$ would give us the polar angle at point r when the origin is set at r_j. Using

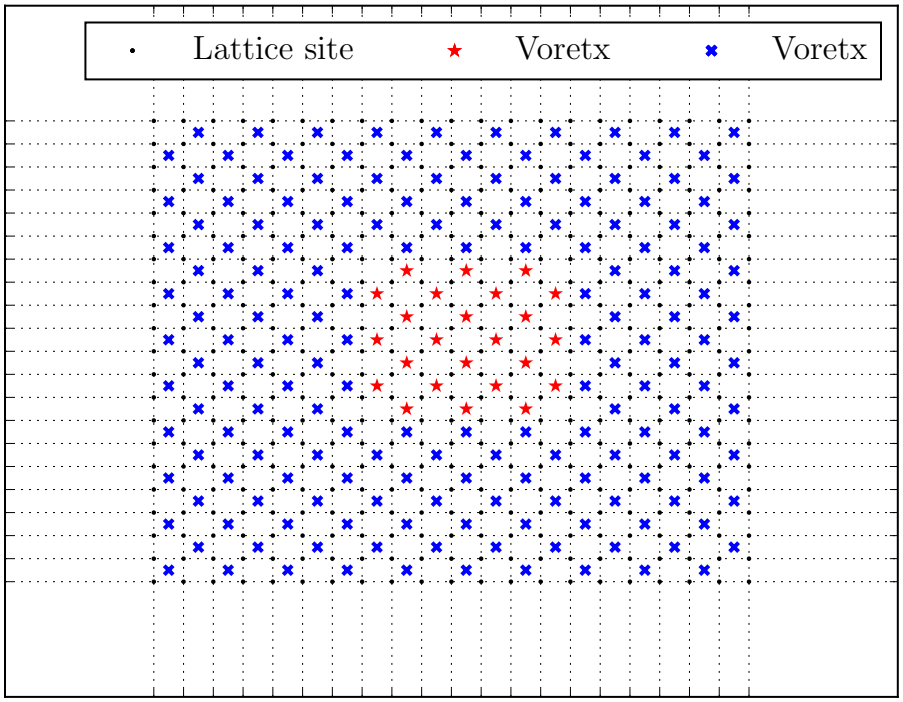

Figure 5.2: The configuration of an array vortices with a defect. The effective vorticity for each corner of the defect is $\frac{1}{4}$ and therefore we expect to observe a Majorana zero mode for each of the corners.

numerical calculation one can compute the energy spectrum of the system with the configuration explained above to see if we could observe any Majorana zero modes. In Fig. 5.3 we plotted the energy spectrum with respect to the inverse of the system size. One can notice that the energy spectrum would not show any evidence of Majorana zero modes. Also ground state wavefunction does not indicate presence of the Majorana zero modes (see Fig. 5.4)

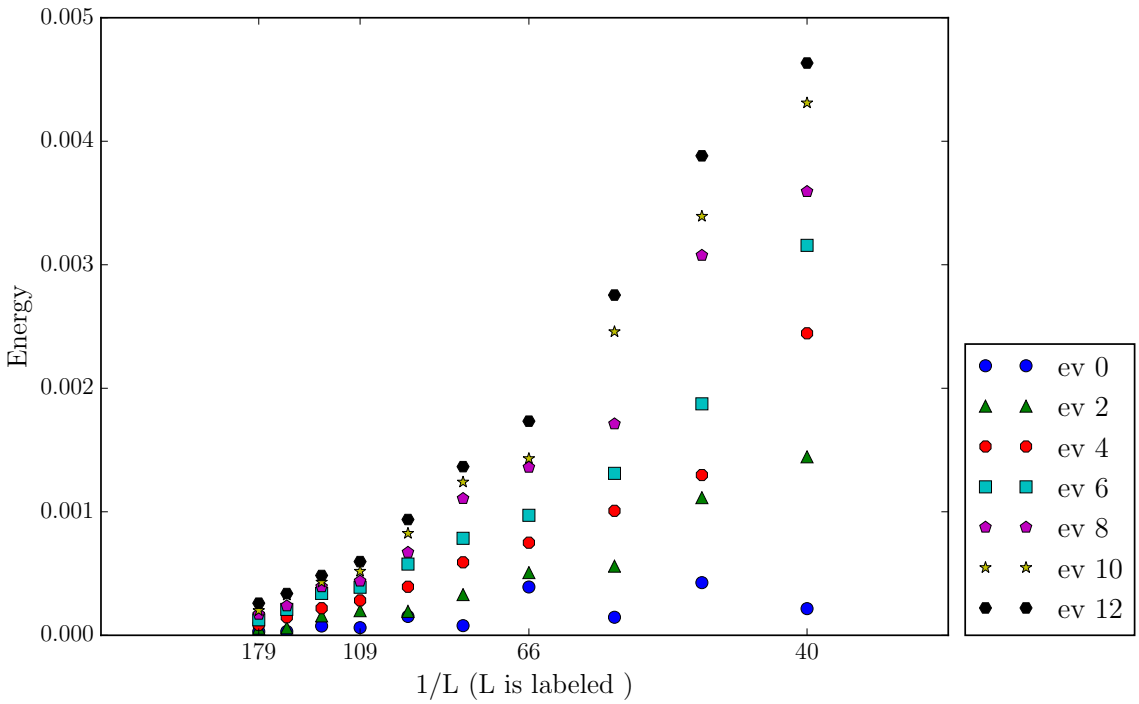

Figure 5.3: The energy spectrum of an array of vortices in a $d + id$ superconductor as a function of $1/L$ where L is the size of the system. The parameter we used are $\mu/t = 2$ and $\Delta_0/(a^2 t) = .2$

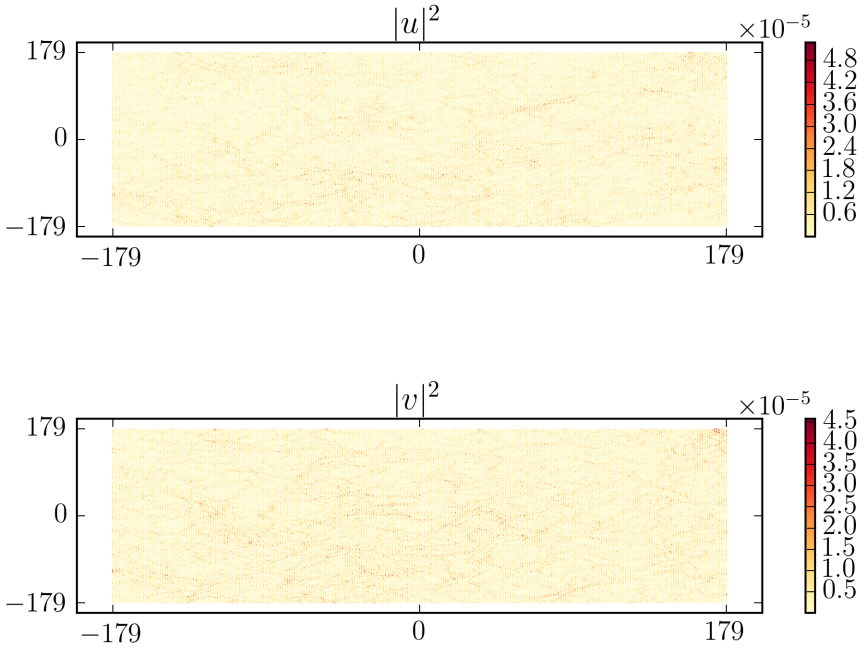

Figure 5.4: The ground state wavefunction of an array of vortices in $d + id$ superconductor. We can not observe any Majorana zero modes in this ground state. The system size is taken to be $L/a = 179$ while the other parameters we used are $\mu/t = 2$ and $\Delta_0/(a^2 t) = .2$

Bibliography

[1] J. Alicea. New directions in the pursuit of Majorana fermions in solid state systems. *Rep. Prog. Phys.*, 75:076501, 2012.

[2] C. W. J. Beenakker. Search for Majorana fermions in superconductors. *Annu. Rev. Condens. Matter Phys.*, 4:113, 2013.

[3] Martin Leijnse and Karsten Flensberg. Introduction to topological superconductivity and majorana fermions. *Semiconductor Science and Technology*, 27(12):124003, 2012.

[4] D. A. Ivanov. Non-Abelian statistics of half-quantum vortices in p-wave superconductors. *Phys. Rev. Lett.*, 86:268–271, 2001.

[5] Chetan Nayak, Steven H. Simon, Ady Stern, Michael Freedman, and Sankar Das Sarma. Non-Abelian anyons and topological quantum computation. *Rev. Mod. Phys.*, 80:1083–1159, 2008.

[6] Ady Stern. Anyons and the quantum hall effect—a pedagogical review. *Annals of Physics*, 323(1):204 – 249, 2008. January Special Issue 2008.

[7] A. R. Akhmerov. Topological quantum computation away from the ground state using majorana fermions. *Phys. Rev. B*, 82:020509, Jul 2010.

[8] G. Volovik. Fermion zero modes on vortices in chiral superconductors. *JETP Letters*, 70:609–614, 1999. [*Pisma Zh. Eksp. Teor. Fiz.* **70**, 601 (1999)].

[9] N. Read and Dmitry Green. Paired states of fermions in two dimensions with breaking of parity and time-reversal symmetries and the fractional quantum Hall effect. *Phys. Rev. B*, 61:10267–10297, 2000.

[10] Andrew Peter Mackenzie and Yoshiteru Maeno. The superconductivity of $\mathrm{sr_2ruo_4}$ and the physics of spin-triplet pairing. *Rev. Mod. Phys.*, 75:657–712, May 2003.

[11] Suk Bum Chung, Hendrik Bluhm, and Eun-Ah Kim. Stability of half-quantum vortices in p_x+ip_y superconductors. *Phys. Rev. Lett.*, 99(19):197002, 2007.

[12] J. Jang, D. G. Ferguson, V. Vakaryuk, R. Budakian, S. B. Chung, P. M. Goldbart, and Y. Maeno. Observation of half-height magnetization steps in Sr_2RuO_4. *Science*, 331(6014):186–188, 2011.

[13] Hae-Young Kee and Manfred Sigrist. Releasing half-quantum vortices via the coupling of spin polarization, charge- and spin-current. 2013.

[14] J. Bardeen, L. N. Cooper, and J. R. Schrieffer. Theory of superconductivity. *Phys. Rev.*, 108:1175–1204, Dec 1957.

[15] J. Bardeen, L. N. Cooper, and J. R. Schrieffer. Microscopic theory of superconductivity. *Phys. Rev.*, 106:162–164, Apr 1957.

[16] C. Caroli, P. G. De Gennes, and J. Matricon. Bound fermion states on a vortex line in a type II superconductor. *Physics Letters*, 9(4):307–309, 1964.

[17] G. E. Volovik. An analog of the quantum hall effect in a superfluid 3he film. *Sov. Phys. JETP, 67, 1804*, 1988.

[18] Eytan Grosfeld and Ady Stern. Observing Majorana bound states of Josephson vortices in topological superconductors. *PNAS*, 108:11810–11814, 2011.

[19] Paul Fendley, Matthew P. A. Fisher, and Chetan Nayak. Edge states and tunneling of non-Abelian quasiparticles in the $\nu = 5/2$ quantum Hall state and p+ip superconductors. *Phys. Rev. B*, 75:045317, 2007.

[20] Michael Stone and Rahul Roy. Edge modes, edge currents, and gauge invariance in p_x+ip_y superfluids and superconductors. *Phys. Rev. B*, 69:184511, May 2004.

[21] J. D. Hunter. Matplotlib: A 2d graphics environment. *Computing In Science & Engineering*, 9(3):90–95, 2007.

[22] Bela Bauer, Roman M. Lutchyn, Matthew B. Hastings, and Matthias Troyer. Effect of thermal fluctuations in topological p-wave superconductors. *Phys. Rev. B*, 87:014503, Jan 2013.

[23] Manfred Sigrist and Kazuo Ueda. Phenomenological theory of unconventional superconductivity. *Rev. Mod. Phys.*, 63:239–311, Apr 1991.

[24] D. A. Ivanov. The energy-level statistics in the core of a vortex in a p-wave superconductor. *eprint arXiv:cond-mat/9911147*, November 1999.

[25] Sankar Das Sarma, Chetan Nayak, and Sumanta Tewari. Proposal to stabilize and detect half-quantum vortices in strontium ruthenate thin films: Non-Abelian braiding statistics of vortices in a $p_x + ip_y$ superconductor. *Phys. Rev. B*, 73:220502, 2006.

[26] Meng Cheng, Roman M. Lutchyn, Victor Galitski, and S. Das Sarma. Splitting of Majorana-fermion modes due to intervortex tunneling in a $p_x + ip_y$ superconductor. *Phys. Rev. Lett.*, 103:107001, 2009.

[27] Rahul Roy. Topological Majorana and Dirac zero modes in superconducting vortex cores. *Phys. Rev. Lett.*, 105:186401, Oct 2010.

[28] Sumanta Tewari, S. Das Sarma, and Dung-Hai Lee. Index theorem for the zero modes of Majorana fermion vortices in chiral p-wave superconductors. *Phys. Rev. Lett.*, 99(3):037001, 2007.

[29] Takahiro Fukui and Takanori Fujiwara. z_2 index theorem for majorana zero modes in a class d topological superconductor. *Phys. Rev. B*, 82:184536, Nov 2010.